POLITECNICO DI TORINO

Master's degree in Mechatronic Engineering

A Review of Multi-Phase Permanent-Magnet Synchronous Motors

Supervisor

Prof. Andrea TONOLI

Co-supervisor

Prof. *Renato* GALLUZZI

Candidate

Alessandra Maria BOSCO

Academic Year 2023-2024

Abstract

High efficiency, high power levels, reliability are demands that have led many researchers to dive into the field of multiphase motors. Especially the world of the electric car, a growing trend, is pushing for increasingly high-performance solutions that will facilitate their widespread use.
The purpose of this work is to provide an overview of the multi-phase permanent magnet synchronous motor and to show what steps are needed to calculate the basic parameters to highlight some of the benefits. In order to understand how a permanent-magnet motor works, a review of three-phase motors is presented, specifying transformations that allow simplified modeling to control them. Emphasis is placed on five-phase, six-phase and nine-phase motors, then proceeding to highlight what are the topologies of multiphase drives based on the structure and number of levels of their respective output voltage. To obtain a more complete review, multiphase induction and reluctance motors are mentioned.
Lastly, the covered topologies based on the number and arrangement of the phases are summarized and not only the benefits of the multi-phase machine are highlighted but also the advantages and disadvantages in using different multiphase drive.

Table of contents

Candidate 1

Abstract **2**

Acronyms ..... **iii**

List of Symbols ..... **vi**

List of Tables ..... **x**

List of Figures ..... **xi**

Chapter 1 ..... **1**

Some steps up to multi-phase permanent magnet synchronous motors **1**

1.1 Aim of the Thesis 3

1.2 Thesis Organization 3

Chapter 2 ..... **5**

Fundamentals of PMSM **5**

2.1 Theoretical basic concepts 5

2.1.1 Rotating magnetic field 6

2.2 Key characteristics of PMSM 9

2.2.1 Line-start PMSM 13

2.3 Three-phases PMSM 14

2.3.1 Park Transformation: dq model 17

Chapter 3 ..... **26**

Multi-phase PMSM **26**

3.1 How many phases 27

3.1.1 Five phase PMSM 29

3.1.2 Six phase PMSM 38

3.1.3 Nine phase PMSM 48

Chapter 4 ..... **52**

Multiphase drive 52
4.1 DC link 53
4.2 Power electronic converters 60
4.2.1 Topologies and modulation 64
4.3 Power semiconductor device 70

Chapter 5 72

Other multi-phase motors 72
5.1 Induction motor 72
5.1.1 Seven phase induction motor 73
5.2 Reluctance motor 75
5.3 Axial flux motor 78

Chapter 6 80

Discussion 80
6.1 Field of application 82
6.2 Summarizing table 86
6.3 Conclusion 88

Bibliography 90

Acronyms

1Ph fault
One phase fault

A2Ph fault
Two phase fault

AC
Alternating current

ASIC
Application Specific Integrated Circuits

BLDC
Brushless DC motor

BPMSM
Buried permanent magnet synchronous motor

CP
Consequent pole

CPWM
Carrier based pulse width modulation

DC
Direct current

ECM
electronically controlled motor

EMI
electromagnetic interference

e.m.f
Electromotive force

EV
Electric vehicle

FOC
Field oriented control

FP-PMSM
Five-phase permanent magnet synchronous motor

FSCW
Fractional slot concentrated winding

EV
Electric vehicle

HEV
Hybrid electric vehicle

PHEV
Plug-in hybrid electric vehicle

IM
Induction machine

IPM
Internal permanent magnet

IPMSM
Interior permanent magnet synchronous motor

LSPMSM
Line-start permanent magnet synchronous motor

MMF
Magnetomotive force

MPD
Multiphase drive

MSRM
Multi-phase Switched Reluctance Motors

MTPA
maximum torque per ampere

MTPV
maximum torque per volt

NA2Ph fault
Non adiacent phase fault

NDSDSMFP-PMSM
Novel dual stator delta-shaped magnet five-phase permanent magnet synchronous motor PMSM

NPC
neutral point clamped inverter

PM
Permanent magnet

PMSM
Permanent magnet synchronous motor

SPM
Surface mounted permanent magnet

SRM
Switched Reluctance Motors

SVPMWM
Space vector pulse width modulation

SVM
Space vector modulation

VCT
Vector classification technique

VSD
Vector space decomposition

List of Symbols

A_1
Distribution of magnetomotive force (MMF) in the first winding

A_2
Distribution of magnetomotive force (MMF) in the second winding

A_3
Distribution of magnetomotive force (MMF) in the third winding

B
Magnetic flux density

B_m
Friction coefficient

C_{min}
Dc link capacitance

d_3-q_3
Direct and quadrature components rotating at three times the synchronous speed

e
Electromotive force

$F_{\varphi 1}$
Fundamental amplitude of MMF

F_-
Negative sequence component of MMF

g
Number of group

H
Magnetic field

I
Current

$\boldsymbol{i_{abc}}$
Current vector in abc frame

$\boldsymbol{i_d}$
Current in the d-axis

$\boldsymbol{i_q}$
Current in the q-axis

$\mathbf{i_s}$
Stator current

$\boldsymbol{J}$
Flux density vector or Moment of inertia

K
Interleaving angle

$\boldsymbol{L_a}$
Self-inductance for winding a

$\boldsymbol{L_b}$
Self-inductance for winding b

$\boldsymbol{L_c}$
Self-inductance for winding c

$\boldsymbol{L_d}$
d-axis inductance

$\boldsymbol{L_q}$
q-axis inductance

$\boldsymbol{M_{ab}}$
Mutual inductance between windings a and b

$\boldsymbol{M_{ac}}$
Mutual inductance between windings a and c

$\boldsymbol{M_{ba}}$
Mutual inductance between windings b and a

M_{bc}
Mutual inductance between windings b and c

M_{ca}
Mutual inductance between windings c and a

M_{cb}
Mutual inductance between windings c and b

N
Number of turns of a coil

p
Pole pairs

P_m
Mechanical power

Q
Number of poles

R
Resistance

S
Surface enclosed by l

T
Torque

T_e
Electromagnetic torque

T_l
Load torque

T_{pc}
Clarke-Park transformation matrix

$V_{ppripple}$
peak-to-peak dc link voltage ripple

θ_e

Position of the rotor axis with respect to the stationary axis α

$\boldsymbol{\omega}$
Angular velocity

$\boldsymbol{\omega_s}$
Synchronous speed

$\boldsymbol{v_{abc}}$
Voltage vector in abc frame

$\boldsymbol{v_d}$
Voltage in the d-axis

$\boldsymbol{v_q}$
Voltage in the q-axis

$\boldsymbol{v_s}$
Stator voltage

$\boldsymbol{V_{am}}$
Maximum available output voltage of the inverter

$\boldsymbol{WBG}$
wide bandgap

$\boldsymbol{\lambda_p}$
Permanent magnet flux linkage

$\boldsymbol{\lambda_{p,abc}}$
Permanent-magnet flux linkage vector in abc frame

$\boldsymbol{\psi_M}$
Permanent magnet flux linkage

$\boldsymbol{\Phi}$
phase shift between output voltage and output current of the inverter

$\boldsymbol{\theta}$
electrical phase shift between phases

List of Tables

Table 1:Saliency 22
Table 2:DC-link capacitor RMS ratings comparison for different phase number [83] 59
Table 3: Overview of main advantages of multiphase-machine-based drives 86
Table 4: Overview of inverter topologies 87
Table 5: Comparison between different type of machine 88

List of Figures

Figure 1: Lorentz's law [121] 6
Figure 2: Three Phase winding [89] 8
Figure 3:Three-phase PMSM [108] 10
Figure 4: Rotor topologies for PM motors. (a) SPM. (b) Conventional IPM.[12]. 11
Figure 5: Concentric winding [10] 12
Figure 6:Distributed winding [10] 12
Figure 7: Star connection [97] 15
Figure 8:3-phase PMSM electrical structure [96] 17
Figure 9: Clarke transformation [126] 18
Figure 10:Park transformation [126] 18
Figure 11:Torque-speed characteristic [59] 23
Figure 12:Block scheme of the MTPA control strategy [17] 24
Figure 13: (a) Three separate three-phase windings displaced by 20 electrical degrees. (b) Nine-phase, 40 electrical degree winding distribution. [49] 28
Figure 14:Multiphase machine drive [51] 29
Figure 15: Main circuit of the five-phase H-bridge inverter carried with PMSM [53] 30
Figure 16: d1 -q1 and d3 -q3 space [60] 32
Figure 17:Open-circuit fault conditions of a star-connected five-phase machine from left to right: 1Ph fault, A2Ph fault, and NA2Ph fault [95] 34
Figure 18: phase diagram of phase currents with phase an open fault [53] 35
Figure 19:5-phase where teeth coil has its own intelligent full-bridge module [92] 36
Figure 20: Rotor with shaft [92] 37
Figure 21: Model of NDSDSMFP-PMSM. [57] 38
Figure 22:Winding configurations for 24 slots/20 poles: a) 3-ph; b) 6-ph [73] 39
Figure 23: Electromagnetic torque versus rotor position in the steady state rated operating condition [73] 40
Figure 24:. Configuration of asymmetric six-phase PMSM drive [74] 41
Figure 25: The current phasor diagram after C1 phase open [69] 45
Figure 26:. Fault tolerant drive topologies: Y-topologies (left) and H-topologies (right) [99] 47
Figure 27: DSDRSPIS-PMSM [68] 47
Figure 28: Winding changes in symmetrical fault derating operation [78] 48
Figure 29: split phase configuration of nine-phase winding [76] 49
Figure 30: Winding structure and H-bridge drives of Nine-phase PMSM [81] 51
Figure 31: (a) Phasor diagram of nine-phase winding and (b) winding sets [15] 51

Figure 32: Block diagram of Battery connected multi-level inverter fed PMSM [103].....53
Figure 33:. Electric vehicle with cascaded bidirectional DC-DC converter plus 3-phase voltage source inverter drive system [106].....54
Figure 34:Generic DC link capacitor design flow chart [100].....56
Figure 35: Required dc-link capacitance for different MPDs [48].....58
Figure 36: Conventional multiphase topology with single neutral point [105].....61
Figure 37: Multiphase topology with multiple single-phase units. [105].....61
Figure 38: Multiphase topology with multiple three-phase units [105].....62
Figure 39: Phase currents in p.u. for different MPDs [48].....63
Figure 40: Two-level inverter-fed six-phase machine [48].....64
Figure 41:Five-leg inverter topology [48].....67
Figure 42: Dual-supply, inverter-fed, open-end, winding six-phase machine I [48].....67
Figure 43:Dual-supply, inverter-fed, open-end, winding six-phase machine III [48].....67
Figure 44:NPC-fed, six-phase machine [48].....68
Figure 45: NPC three-level inverters fed dual-three phase PMSM [113].....70
Figure 46: Seven-phase voltage source inverter [115].....73
Figure 47: The arrangement of (a) three-phase SRM and (b) six-phase SRM in NS mode [119].....77
Figure 48: Example of EVs on the market from 2010 to 2020, includingtheir model, motor categories, and power [124].....83
Figure 49: Configuration with combined ultracapacitor and battery [123].....85
Figure 50:EV on-board architecture [24].....85
Figure 51:Conceptual map of the topologies covered.....86

Chapter 1

Some steps up to multi-phase permanent magnet synchronous motors

Over the past two centuries, electric motors have attracted interest and then found use in a myriad of applications.

Since 1830 so many patents have been published that it becomes difficult to classify the huge number of motor types and variations.

It is possible to date the first U.S. patent on electric motors, in 1837, published by inventor Thomas Davenport; or Friedrich August Haselwander, who first developed, in 1887, the three-phase synchronous motor. Perhaps best known is N. Tesla (1856-1943), who filed several patents, including one for a three-phase induction motor, like today's motor.

In 1962, TG Wilson and PH Trickey invented the first brushless DC (BLDC) motor, which they called "DC motors with solid-state commutation." [28] making the use of physical commutators unnecessary and thus marking a fundamental step in the use of electric motors.

All types of motors studied and, on the market, have different advantages and disadvantages, and the most suitable solution is chosen considering the requirements for the specific situation.

For example, unlike conveyors, motor drives in electric vehicles (EVs) require different characteristics, such as high rate of acceleration and deceleration or high torque at low speed. [6].

Compared with other electric machines, permanent magnet (PM) machines combine the advantages of high efficiency (due to the absence of losses in the

rotor), power factor and torque density, high overload capacity, robustness, low maintenance, compactness, and low weight [1], features required of an electric traction machine. [2].

Another reason to speak about PM motors is the absence of external excitation.

The Permanent Magnet Synchronous Motors (PMSMs) have some advantages over asynchronous motors. PMSMs provide a higher power density for their size than the asynchronous because, using a PMSM the rotor flux is already established by the permanent magnets on the rotor while using asynchronous motors, some of the stator current is needed to "induce" the rotor current to produce the rotor flux, which is the reasons why they are called induction motors (IMs).[3].

If induction motors have dominated the drive market by replacing the DC motor in high-performance applications, PMSMs have gained ground starting with the introduction of new materials such as neodymium-iron-boron (NdFeB) in 1983 [7], or samarium-cobalt (SmCo).[4].

However, PM excitation has some disadvantages, such as the risk of demagnetization at high temperatures [1] and the cost of permanent magnets, as the latter are usually made of rare material and their price is increasing.

Nevertheless, several studies present new techniques for PM machines with simple concentrated windings to reduce the amount of magnetic material used. [4].

Permanent magnet machines are used in many applications and sometimes good fault-tolerance capability is required for some safety-critical applications. To meet this need, multiphase (>3) machines can be used, which offer greater freedom in fault handling and have inherent advantages.[5].

Multi-phase stator topologies mainly have some advantages in terms of power segmentation, reliability, and performance, whereas machine structure and construction technology may remain unchanged compared to three-phase design, unless it comes to very high-power electric machines, where adopting an n-phase stator configuration may have considerable “structural” or “constructive” impact.[18].

1.1 Aim of the Thesis

As the power level increases, the adoption of multiphase motors allows higher power levels to be achieved by dividing the required power among more phases, more than the conventional three phases, and allows the use of power electronic converters with a limited power range to drive the multiphase machine. [19].
The specific application areas are the main motivation for this growing interest in the multi-phase machine. Electric ship propulsion, locomotive traction, electric and hybrid electric vehicles, more-electric aircraft, and high-power industrial applications can be considered as the main applications [21].
Some of the advantages listed above highlight how a discussion on multiphase PMSM can be useful. The objective of this work is therefore to proceed step by step to the definition of the intrinsic advantages of this machine, like the fault tolerance capability, and those that derive from it, such as for example the dc-link improvement or the inverter improvement.

1.2 Thesis Organization

Chapter 1 provides a historical overview of electric motors, emphasizing the relevant aspects of permanent magnet synchronous motors. presents in the first instance PMSM advantages, material challenges, and introduces multi-phase stator topologies.
Chapter 2 serves as an introduction to understanding motor presenting a review of three-phase motors and transformations that allow for simplified modeling, Clarke-Park transformation. In addition, the chapter explores different configurations based on winding in the stator and permanent magnets in the rotor.
Chapter 3 presents various configurations of multi-phase permanent magnet synchronous motors, focusing on five-phase, six-phase, and nine-phase designs. The discussion includes the advantages of segmented five-phase PMSMs, the benefits of the asymmetric six-phase motor in reducing torque pulsation. Additionally, the chapter presents the vector space decomposition, the modelling and torque

calculations for the complex nine-phase PMSMs. Contents highlight fault tolerance, robustness, and efficiency in various motor applications.

Chapter 4 defines Multiphase Motor Drives advantages over traditional three-phase systems, emphasizing torque ripple reduction and increased reliability. Specifies the crucial role of the DC link, showing processes and capacitor sizing considerations. The chapter also explores power electronic converters, highlighting different topologies, modulation techniques. Overall, it provides a review design and optimization of multiphase systems for enhanced motor performance.

Chapter 5 explores multi-phase motors, starting with the induction motor's operation and the growing interest in multi-phase configurations. It introduces the seven-phase induction motor. The chapter then deals with the switched reluctance motor (SRM), discussing even and odd-numbered phase SRMs and their characteristics. The discussion includes a comparison of four, five, and six-stage SRMs and concludes by emphasizing the advantages of choosing a specific phase number based on application requirements. Permanent magnet machines can be divided into two primary categories based on the direction of the flux passing through the machine's air gap so the axial flux machines are presented.

Chapter 6 presents PMSM in vehicle traction, emphasizing efficiency and reduced emissions. It discusses inverter configurations and highlights the evolution of hybrid vehicles and the application of multi-phase drives in automotive for enhanced reliability and efficiency. It also applies to provide a comparison of the different solutions presented.

Chapter 2
Fundamentals of PMSM

2.1 Theoretical basic concepts

Before going into some detail about multiphase synchronous machines, it is necessary to review the laws of electromagnetism that will enable us to understand the working principle of such machines.

The most important laws for electrical motors are:

- Ampère's law: the electric current through a conductor produces a magnetic field. The line integral of the vector H around the closed line l is equal to the flux of the density vector J through the surface S enclosed by l.

$$\int_l \overline{H}\overline{dl} = \int_S \overline{J}\overline{dS} \tag{2.1}$$

- Constitutive equation: the magnetic field H produces a flux density B.

$$B = \mu H = \mu_r \mu_0 H \tag{2.2}$$

Where μ_r is the relative permeability and μ_0 is the vacuum permeability

- Hopkinson law is named in honor of the British physicist and engineer who patented the three-phase system for generating and distributing electricity. Hopkinson law, magnetic equivalent of Ohm's law, links the Magneto Motive Force (m.m.f.) with the reluctance of the magnetic circuit and the produces flux.

$$NI = R\Phi \tag{2.3}$$

where N is the number of turns of a coil and I the current flowing in it.

- Lenz's law: if a linked magnetic flux λ varies in time an electromotive force is created (Faraday's law). The induced electromotive force (emf) creates a current that opposes to the flux variation.

$$e = \pm \frac{d\lambda}{dt} \tag{2.4}$$

- Lorentz's law for force: if a current I flows through a rectilinear conductor in a region where B field exists then a force is created, which has direction perpendicular to the plane formed by B and I (*figure 1*).

$$dF = \left(\bar{dl} \wedge \bar{B}\right) I \tag{2.5}$$

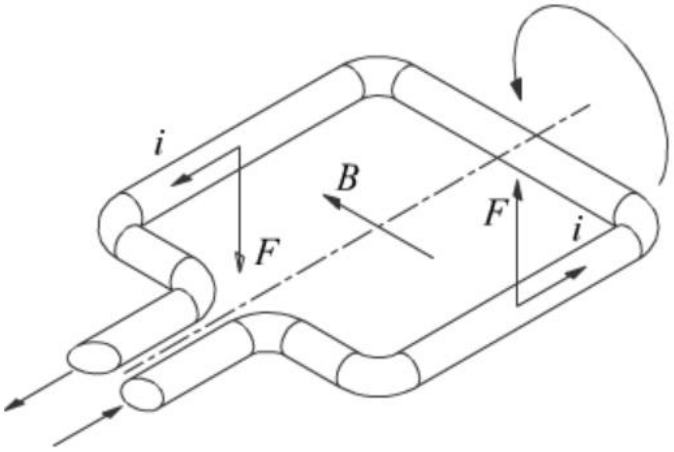

Figure 1: Lorentz's law [121]

2.1.1 Rotating magnetic field

Whether or not he patented his discoveries, in 1885, Galileo Ferraris demonstrated the existence of the rotating magnetic field by using two fixed coils perpendicular to each other, through which circulated two alternating currents of the same frequency

and offset by 90°.[8]-[9]. Patent later published in 1888 by Nikola Tesla.
To generate a rotating magnetic field, multiple (more than one) spatially displaced windings crossed by time-displaced currents are required.
Considering three windings (figure *2*) space-displaced of 120° and crossed by currents time-displaced of 120° three distributions of m.m.f are produced:

$$A_R(\alpha, t) = N_{eq} \sin(\alpha)\, i_R(t) \tag{2.6}$$

$$A_B(\alpha, t) = N_{eq} \sin(\alpha - \frac{2\pi}{3})\, i_B(t) \tag{2.7}$$

$$A_Y(\alpha, t) = N_{eq} \sin(\alpha - \frac{4\pi}{3})\, i_Y(t) \tag{2.8}$$

Where:

- Each winding has the same number of turns, the same number of pole pairs and therefore the same equivalent number of turns N_{eq}.
- The flowing currents make a symmetrical set:

$$i_R = \hat{I} \cos(\omega t) \tag{2.9}$$

$$i_B = \hat{I} \cos(\omega t - \frac{2\pi}{3}) \tag{2.10}$$

$$i_Y = \hat{I} \cos(\omega t - \frac{4\pi}{3}) \tag{2.11}$$

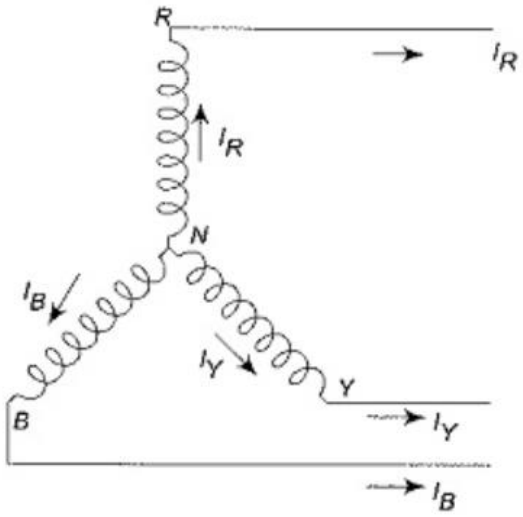

Figure 2: Three Phase winding [89]

The resulting fundamental m.m.f. $A_t(\alpha,t)$ produces a rotating magnetic field $H_t(\alpha,t)$ and the related rotating magnetic flux density distribution $B_t(\alpha,t)$:

$$A_t(\alpha,t) = \frac{3}{2} N_{eq} \hat{I} \sin(\alpha - \omega t) \tag{2.12}$$

$$H_t(\alpha,t) = \frac{3N_{eq}}{2l_t} \hat{I} \sin(\alpha - \omega t) \tag{2.13}$$

$$B_t(\alpha,t) = \frac{3N_{eq}}{2l_t} \mu_0 \hat{I} \sin(\alpha - \omega t) \tag{2.14}$$

Where l_t la the air gap length.

As previously stated, a rotating magnetic field is obtainable not only from a three-phase system but can be generated by an n-phase (n not equal to one) system with n currents phase-shifted by $\frac{2\pi}{n}$ electrical degrees passing through n windings with sinusoidal distribution phase-shifted by $\frac{2\pi}{n}$ mechanical degrees.

These are the key formulas essential in understanding methods for producing or exploiting electricity, as for example the object of this work, the multi-phase

permanent magnet synchronous motor.

2.2 Key characteristics of PMSM

The main characteristic of synchronous motors is that the rotational speed of the rotor is equal to the frequency of the supply voltage divided by the number of pole pairs.[7].

$$\omega_{mech} = \frac{\omega}{p} \tag{2.15}$$

In other word, the mechanical speed is equal to the speed of the stator rotating magnetic field.

The speed of the stator rotating magnetic speed is called "synchronous speed". In the case of synchronous machine, the relative difference between the synchronous speed and the mechanical speed of the rotor is therefore equal to zero. The relative difference is called "slip". It is possible to use the absolute slip (2.16) or the relative slip (2.17):

$$s = \omega_s - \omega_m \, [rad/s] \tag{2.16}$$

$$s = \frac{\omega_s - \omega_m}{\omega_s} \tag{2.17}$$

The revolving stator m.m.f. is the result of injecting a set of polyphase currents phase shifted from each other by the same amount of phase shift between the multi-phase windings. [10]. In case of three phase PMSM the currents in the three windings are

120° out of phase, the magnetic fields produced will also be 120° out of phase.[31].
The operating principle of a synchronous motor is quite like that of an asynchronous motor. The coils, inserted into slot of the stator core, generate a rotating magnetic field whose polar expansions interact with those of the rotor, causing slip and thus achieving rotation. The purpose of the rotor is to create an excitation magnetic field either through permanent magnets or DC excitation. In PMSM the north pole of the rotating field in the stator attracts the south pole of the magnet, and simultaneously the south pole of rotating magnetic field attracts the north pole of the magnet.
In the asynchronous machine, instead, the field produced by the rotor is due to induced currents in the rotor windings (hence called "induction" machine).
The use of permanent magnets to produce the rotor field is advantageous because it avoids the use of brushes and commutators, which is why the permanent magnet synchronous motor (*figure 3*) is said to be brushless.

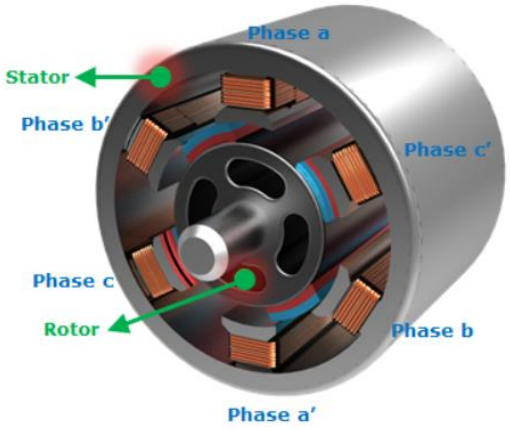

Figure 3:Three-phase PMSM [108]

This leads to some advantages: rotor reduced losses associated to the induced current, the consequent increase in efficiency and the reduction of required maintenance due to the absence of the brushes and commutators.

Based on the shape and position of the permanent magnet in the rotor there are two main topologies of permanent magnet rotor (of which there are modified versions): surface mounted permanent magnet (SPM) in *figure. 4(a)* and internal permanent magnet (IPM) in *figure. 4(b).*

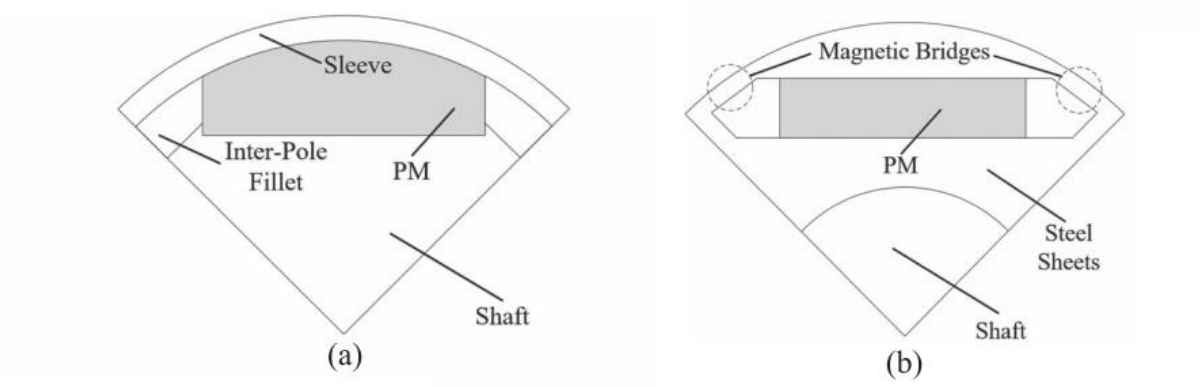

Figure 4: Rotor topologies for PM motors. (a) SPM. (b) Conventional IPM.[12].

In the surface mounted PMSMs the permanent magnets are exposed to the air gap. The interior PMSM (IPMSM) has its magnets buried inside the rotor.[16]

From the comparison with finite element analysis, it can be concluded that the IPM motor has similar electromagnetic performance as the SPM motor in high-speed operations, while the cost and torque per weight of the IPM are higher than those of the SPM motor. However, the rotor structure is not as robust and is subject to irreversible demagnetization.[12].

Important to highlight how the way the conductors are placed in the stator determines not only the m.m.f. distribution at the air gap, but also e.m.f. induced in the winding, that is proportional to the product of the rotational frequency and the flux in the air gap.

The m.m.f. produced by the coil has a rectangular distribution with a fundamental component useful for torque, but there are also harmonics that produce losses. One of the requirements in motor design is to minimize these harmonics to increase efficiency (reducing losses).

The first categorization of winding in the stator is based on how the coils are

distributed in the slots. To obtain a sinusoidal distribution of m.m.f. regardless of the number of phases, we distinguish: concentric winding and distributed winding.

Before introducing these two typologies, two parameters need to be defined: pole pitch and coil pitch.

The pole pitch is defined as the distance measured in terms of armature slots that come between two adjacent pole centers. Pole Pitch is equal to the total number of armature slots divided by the total number of poles in the machine.

Coil pitch is defined as the peripheral distance between two sides of a coil also measured in terms of the number of armature slots between them.

In concentric winding (*figure 5*) the windings are distributed in the slots with different coil pitches within a pole pitch, while in distributed winding (*figure 6*) the number of conductors in each slot is the same and the coils pitch is constant for all coils. Fractional slot concentrated winding (FSCW) is an alternative where every coil is wrapped on a tooth [29], avoiding overlap in the end winding not only minimizes the insulation volume but can also potentially enhance power density.[29]

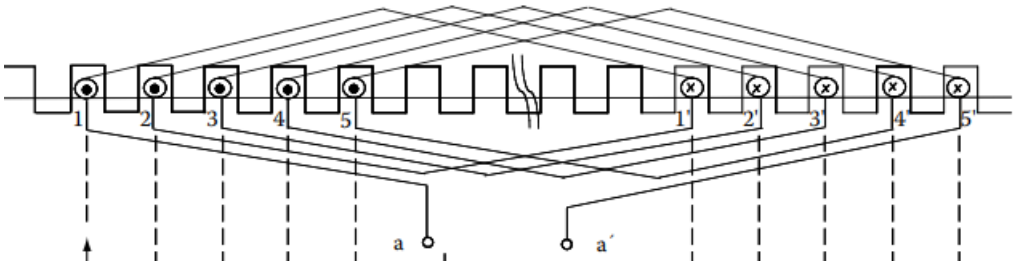

Figure 5: Concentric winding [10]

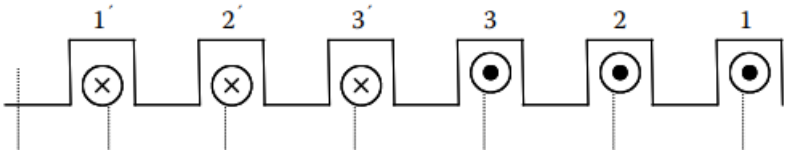

Figure 6:Distributed winding [10]

According to the theory of winding, the number of slots per pole of each phase q can be given as:

$$q = \frac{Q}{2mp} \tag{2.18}$$

where Q represents the number of slots, m is the number of phases and p is the number of pole-pairs. In a distributed overlap winding setup, where q is an integer, the coil pitch is approximately m multiplied by q. However, in a concentrated winding configuration, q is a fraction, and the coil pitch is set to 1. [29].

How the number of slots and poles is chosen affects machine performance, so it is an important parameter in machine design. Winding factor, cogging torque, radial forces, flux attenuation capability are some of the parameters involved.[30]

Additional techniques in control algorithm are used to achieve a more sinusoidal m.m.f., like Field Oriented Control (FOC) that are seen later.

2.2.1 Line-start PMSM

One of the disadvantages of PMSM is the complexity of startup, which with certain arrangements has become yet another strength.

Knowing that torque is produced when the salient field poles of the rotor concatenate with the stator's rotating magnetic field, causing the rotor to rotate at synchronous speed, this implies that application of the stator's supply voltage is unable to produce starting.

To overcome this problem, the cage equipped PM motors, so-called line-start permanent magnet synchronous motors (LSPMSM) have been developed since 1955. [35].

These motors are equipped with a squirrel cage winding, which plays a crucial role in generating torque from a standstill up to the synchronous speed.

These windings are connected to the AC power supply, the rotor starts to rotate due to the interaction of the rotating magnetic field of the stator with the currents induced in the squirrel cage winding, this means that during the startup, this motor behaves like an induction motor.

However, once the synchronous speed is attained, the cage windings cease to

produce electrical torque, as there are no induced voltages at that point.
LSPMSM is widely employed in various industrial applications, particularly in ventilation and fan drives, showing its versatility for different industrial drive motors.[39].
LSPMSM is one of the highest efficiency motors with advantages compared to other types of induction motor such as robust structure and high-power density [34] and compared to simple PMSM thanks to direct starting.
Its distinctive design combines a rotor cage and permanent magnets, optimizing both starting torque and operational efficiency while minimizing losses in rotor bars during synchronous operation.
Another solution is to provide the stator with a variable frequency power supply, via the appropriate inverters. By varying the frequency of the power supply, the rotating magnetic field is generated which rotates at an initially low speed allowing the magnetic field generated by the permanent magnets to link with it; in this way the rotor begins to rotate at the same speed of the rotating field.

2.3 Three-phases PMSM

After a general survey of the permanent-magnet synchronous motor, we turn our attention to three-phase PMSMs, the basis for building a study of multiphase (more than three) motors. Three-phase Permanent Magnet Synchronous Motors (PMSMs) are widely utilized electric motors, celebrated for their efficiency, reliability, and precision control. Below, we provide an overview of key aspects concerning three-phase PMSMs.
PMSMs integrate a rotor equipped with permanent magnets, capable of autonomously generating a magnetic field, obviating the necessity for an external power source.
The stator comprises three sets of windings uniformly distributed around the motor's circumference. These windings are typically configured in a sinusoidal pattern to optimize performance.
Since rotor has no windings, the generation of heat, mainly due to Joule losses, it is only on the stator, where it is easier to dissipate the heat because it is in direct

contact with the environment.

PMSMs operate based on the concept of synchronous rotation, wherein the rotor tries to synchronize itself with the rotating magnetic field generated by the stator windings. The rotor's permanent magnets establish a stable magnetic field, while the stator windings generate a rotating magnetic field when energized with three-phase alternating current (AC).

The interaction between the rotor's magnetic field and the stator's revolving magnetic field results in the production of mechanical torque, pushing the rotor to rotate synchronously at a predetermined speed.

Considering an electric machine having two magnetic poles and which is characterize by a star connection (*figure 7*). Assuming then that is an isotropic machine, it follows that:

- $p = 1$

(2. 19)

- The sum of the three currents must be equal to zero:

$$i_1 + i_2 + i_3 = 0$$

(2. 20)

- Mutual inductances do not depend on the direction:

$$M_{ij} = M_{ji}$$

(2. 21)

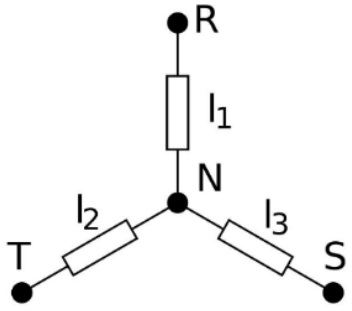

Figure 7: Star connection [97]

The voltage of the three phases is given by:

$$\begin{cases} v_{1N} = R_s i_1 + \dfrac{d\lambda_1}{dt} \\ v_{2N} = R_s i_2 + \dfrac{d\lambda_2}{dt} \\ v_{3N} = R_s i_3 + \dfrac{d\lambda_3}{dt} \end{cases}$$

(2. 22)

The linked flux expression for the i-th phase:

$$\begin{cases} \lambda_1 = L_1 i_1 + M_{12} i_2 + M_{13} i_3 + \lambda_{p1} \\ \lambda_2 = L_2 i_2 + M_{21} i_1 + M_{23} i_3 + \lambda_{p2} \\ \lambda_3 = L_3 i_3 + M_{31} i_1 + M_{32} i_2 + \lambda_{p3} \end{cases}$$

(2. 23)

Where λ_p is the linkage flux due to the permanent magnet established on i-th winding.
Collecting the inductances:

$$L_i - M = \frac{3}{2} L + L_d = L_s$$

(2. 24)

Where L_d is the dispersion matrix.
By rearranging 2.19 it is possible to obtain:

$$[v_{in}] = R_s[i_i] + L_s \frac{d[i_i]}{dt} + \left[\frac{d\lambda_p}{dt}\right]$$

(2. 25)

Where $\frac{d\lambda_p}{dt}$ is the emf.

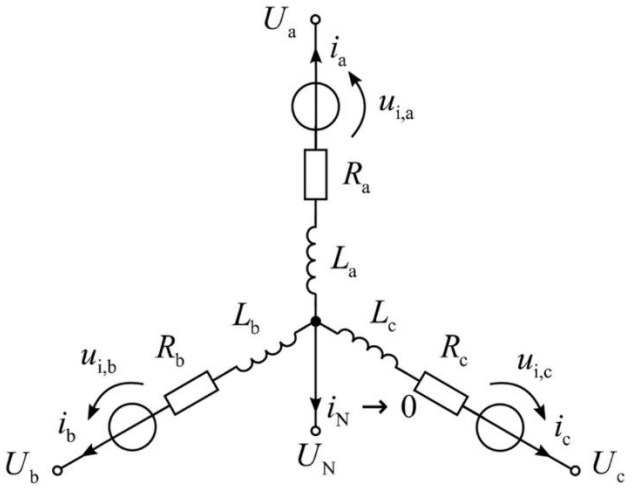

Figure 8:3-phase PMSM electrical structure [96]

In agreement with the expression on the voltage drop across the coil, the three phase PMSM electrical structure is given by *figure* 8.

2.3.1 Park Transformation: dq model

To simplify the modelling, it is common practice to transform system state variables:

1. Clarke's matrix (*figure 9)* enables the conversion of a three-phase system into a two-phase system while retaining the essential characteristics of the original three-phase system. In this process, sinusoidal variables that were initially fixed to the stator reference system become constant variables synchronized with the rotor.
2. The Park matrix (*figure 10*) [37], on the other hand, facilitates the alignment of multiple two-phase systems, each with varying angular positions, to a

common reference system d-q, direct axis and quadrature axis. This transformation simplifies the analysis and the control of the motor by decoupling the torque generation (q-axis) and the magnetizing component (d-axis).

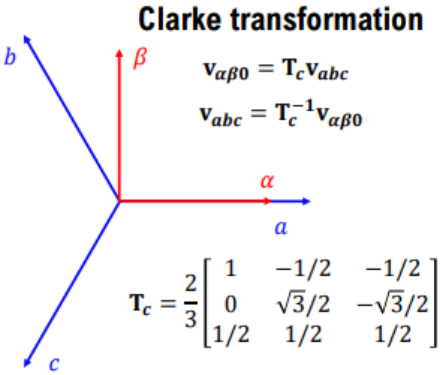

Figure 10:Park transformation [126]

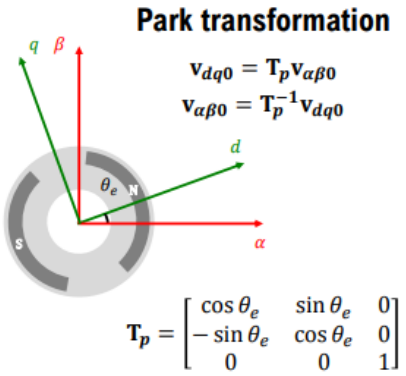

Figure 9: Clarke transformation [126]

The voltage over each stator winding is given by the sum of the voltage drop on the resistance and the induced voltage due to the time-varying flux linkage:

$$v_{abc} = \frac{d\lambda_{abc}}{dt} + R_{abc} i_{abc} \tag{2.26}$$

Flux linkage vector:

$$\lambda_{abc} = \lambda_{p,abc} + L_{abc} i_{abc} \tag{2.27}$$

Where λ_p is the linkage flux due to the permanent magnet established on the

windings.

Permanent-magnet flux linkage vector:

$$\lambda_{p,abc} = \begin{cases} \lambda_p \cos\theta_e \\ \lambda_p \cos(\theta_e - \frac{2}{3}\pi) \\ \lambda_p \cos(\theta_e + \frac{2}{3}\pi) \end{cases}$$

(2. 28)

Where θ_e identifies the position of the rotor axis with respect to the stationary axis α. The inductance matrix is defined as:

$$L_{abc} = \begin{bmatrix} L_a & M_{ab} & M_{ac} \\ M_{ba} & L_b & M_{bc} \\ M_{ca} & M_{cb} & L_c \end{bmatrix}$$

(2. 29)

Where the diagonal elements are given by the self-inductances and the off-diagonal elements are the mutual inductances. The matrix exhibits symmetry because the flux coupling between two windings is equal in both directions.

The resistance matrix is a diagonal matrix where diagonal elements represent the stator resistances that are equal in all windings because stator windings are wound with the same number of turns.

$$R_{abc} = \begin{bmatrix} R & 0 & 0 \\ 0 & R & 0 \\ 0 & 0 & R \end{bmatrix}$$

(2. 30)

It is possible to collect the two transformations in Clarke-Park transformation defined by the matrix:

$$T_{pc} = T_p T_c = \begin{bmatrix} \cos\theta_e & \cos(\theta_e - \frac{2}{3}\pi) & \cos(\theta_e + \frac{2}{3}\pi) \\ -\sin\theta_e & -\sin(\theta_e - \frac{2}{3}\pi) & -\sin(\theta_e + \frac{2}{3}\pi) \\ 1/2 & 1/2 & 1/2 \end{bmatrix}$$

(2. 31)

Knowing that the magnetizing inductance is not constant as the reluctance depends on the position of the rotor, this transformation allows us to obtain a set of equations referring to a reference system that rotates synchronously with the rotor, consequently the inductance matrix becomes constant.

The voltage in dq axes is obtained from:

$$v_{dq0} = T_{pc} \frac{d}{dt}\left(L_{abc} T_{pc}^{-1} i_{dq0} + \lambda_{p,abc}\right) + T_{pc} R_{abc} T_{pc}^{-1} i_{dq0}$$

(2. 32)

In expanded form the voltage in q axis and in d axis is [7]:

$$v_d = L_d \frac{di_d}{dt} + R i_d - p L_q \omega i_q$$

(2. 33)

$$v_q = L_q \frac{di_q}{dt} + R i_q + p L_q \omega i_q + p \lambda_p \omega$$

(2. 34)

The maximum available output voltage of the inverter (V_{am}) represents a constraint for the terminal voltage [46],[14], so that:

$$\sqrt{{v_d}^2 + {v_q}^2} \leq V_{am}$$

(2. 35)

The input power in abc frame is:

$$P_{abc} = {v_{abc}}^T i_{abc}$$

(2. 36)

Respecting the power equivalence, i.e., the power must be the equal in both reference frames:

$$P_{dq0} = \frac{3}{2}{v_{dq0}}^T i_{dq0} =$$

$$= \frac{3}{2}(v_d i_d + v_q i_q) = \frac{3}{2}\left[L_d i_d + L_q i_q \frac{di_q}{dt} + p\left(L_d - L_q\right)\omega i_d i_q + p\lambda_p \omega i_q + R(i_d^2 + i_q^2)\right]$$

(2. 37)

Where:

$$P_m = p\left(L_d - L_q\right)\omega i_d i_q + p\lambda_p \omega i_q$$

(2. 38)

Finally, moving on to the equation on torque and knowing that it is given by the ratio between power in the air gap and angular velocity, we obtain:

$$T = \frac{P_m}{\omega} = \frac{3}{2}p\lambda_p i_q + \frac{3}{2}p(L_d - L_q) i_d i_q$$

(2. 39)

The first term corresponds to “the magnet excitation torque” occurring between i_q and the permanent magnet, while the second term corresponds to “the reluctance torque” due to the difference in d-axis and q-axis reluctance and the consequent inductance.

The torque generation depends also on rotor saliency. Saliency ratio is defined as the ratio of q- axis inductance to d- axis inductance $\left(\frac{L_q}{L_d}\right)$.

As it is said before, PMSM can be divided in two groups, interior PMSM and surface mounted PMSM, depending on the position of the PM. [47]

SPMSM have the capacity to generate only the magnet excitation torque because it is not salient-machine that means it has same d- and q-axis inductance values; IPMSMs are salient machines, and they also produce reluctance torque due to the difference in inductances [45].

Parameter	SPM	IPM
PM flux linkage	$\lambda_p > 0$	$\lambda_p > 0$
Inductance term	$L_d = L_q$	$L_d < L_q$
Machine	Not-salient machine	Salient machine

Table 1:Saliency

The equation of motion is given by:

$$T_e - T_l = J\frac{d\omega}{dt} + B_m\omega \tag{2.40}$$

T_e is electromagnetic torque; T_l is Load torque; J is moment of inertia; B_m is friction factor, coefficient associated with the rotational system of the machine and the mechanical load.

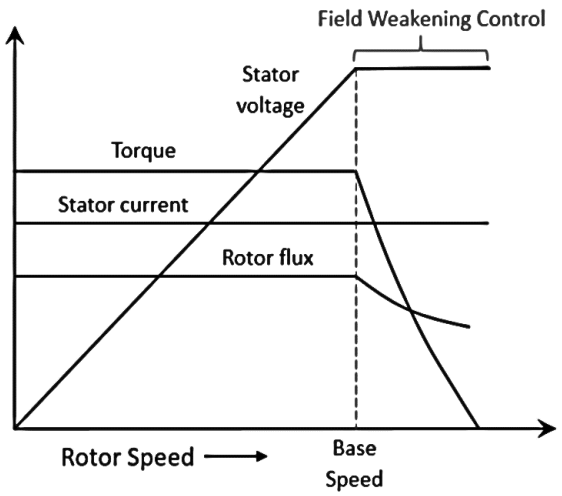

Figure 11:Torque-speed characteristic [59]

The torque is also proportional to the q-axis current, this results in simpler control models [40] which will be dealt with later.

On the contrary, the torque is inversely proportional to the angular speed.

In application such as traction a wide range speed operation is required, to this purpose it is worth highlighting the torque-speed characteristic (*figure 11*) [41].

From zero to a base speed occurs a constant torque region, with an increasing voltage. To reach a maximum operational speed, the motor works in flux-weakening region, with a constant voltage and a decreasing torque.

As can be seen in figure 12, this region is characterized by a constant power range determined by the limitation of energy supply system and motor properties [43].

The base speed is the maximum speed limited by stator voltage, rated current and back-emf. To increase the speed the back-emf required is more than the supply voltage. Reducing the rotor flux it is possible to reach this goal. This operation is known as “field-weakening” control of the motor, indeed, as previously mentioned, "flux weakening", a more precise term as it is not possible to act directly on the rotor field produced by the permanent magnet [44].

It is necessary to counteract the flux in the airgap generated by the magnet acting on the opposite flux induced by the stator current (setting d-axis stator current to a negative value). [44]

The interior PMSM has more flux weakening capability, so it is more suitable for

wide-speed application. The flux of the permanent magnet is less sensitive to the demagnetization and a possible reason is that it is less exposed to the armature winding [42].

Another structure provides less demagnetization risk for the surface magnets and a significant reduction of magnet cost, relevant factor in applications such as automotive. It is known as consequent pole (CP) rotor topology. It improves field weakening capability. Its rotor topology takes advantage of simpler and cheaper construction in addition to wider flux weakening capability than conventional PM motors. The topology is composed of semi-inset type magnets for high-speed protection of the magnets and the laminated iron rotor poles. [15].

Different works present flux weakening control algorithm with maximum torque per ampere (MTPA) control for high-speed operations that requires a mathematical model of the machine. In the MTPA-oriented system (*figure 12*), the speed error, defined as the disparity between the reference speed (ω) and the measured rotor speed (ω) using a resolver, is computed by the "Speed Controller" block. The "MTPA" block determines the instantaneous values of i_d and i_q to maximize electromagnetic torque. These calculated currents are compared in the "Current Controller" block with the actual input currents, resulting in reference values for Park components (v_d and v_q). Subsequently, through inverse Park transformation, these values are reconverted into the original reference system and applied to the motor using PWM techniques. [17]

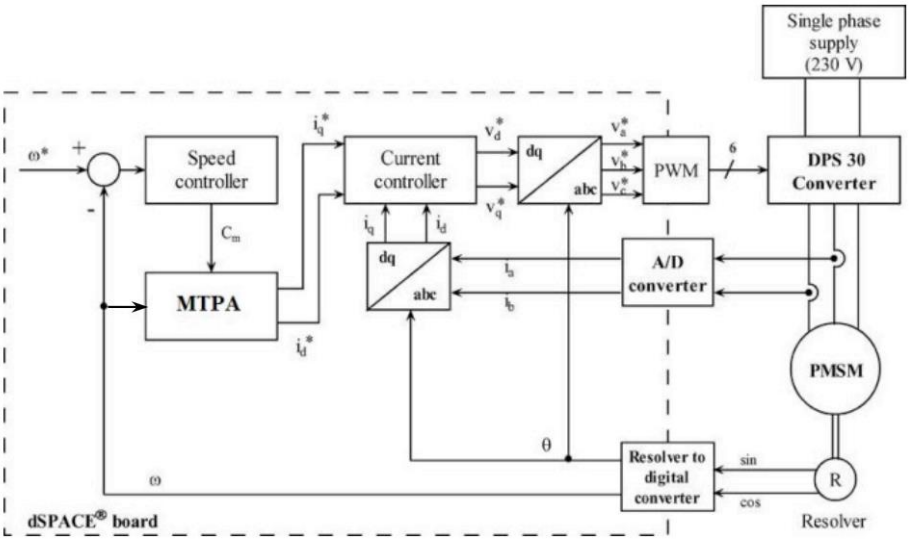

Figure 12:Block scheme of the MTPA control strategy [17]

A relevant tendency in the automotive industry is the need to provide torque assistance and torque boosting in the powertrain. The electric traction requires motors with high torque at low speeds and wide speed range at constant power. So below the nominal speed, the MTPA strategy is used to minimize the required current.[22]

Another strategy is used, whose objective is to maximize the torque obtained from the available voltage. It is imposed the norm of the voltage at the maximum voltage Vmax. This strategy is called MTPV (Maximum Torque Per Volt).[23]

The problem can be written as:

$$V_q, V_q \rightarrow \max T \tag{2.41}$$

$$V_q{}^2 + V_d{}^2 = V_{max}{}^2 \tag{2.42}$$

Chapter 3
Multi-phase PMSM

As it is said before, multi-phase motor drives have several advantages when compared to the standard three-phase motor drives. The main advantage of multiphase drives is the possibility to share the delivered power among more inverter legs, which reduces the current stress of each power device [36], in comparison with a three-phase converter [13].

From the viewpoint of the machine itself, as the power increases, phase current also grows, requiring larger coil cross-sections and fewer turns. Beyond a certain power level, a single turn coil design becomes mandatory, leading to a shift from coil winding to costlier Roebel bar technology. However, adopting an n-phase stator configuration (n>3) reduces phase current by approximately n/3, making it possible to maintain a coil design for the stator winding and avoiding expensive Roebel bars, resulting in significant cost and production time savings [18].

Other potential advantages of multiphase drives over three-phase ones are: lower space harmonic content; reduced torque ripple; smaller rotor harmonic currents; reduced stator copper losses; higher power per rms ampere ratio for the same machine volume; reduced current harmonic content in the dc link in case of voltage source inverter (VSI) fed drives; and higher reliability.[13]

The growing demand for fault-tolerant drives necessitates innovative solutions that avoid the adoption of custom and costly configurations.

In critical applications, the ability to continue to operate under fault conditions is fundamental. Multiphase drives excel in this aspect because of their additional degrees of freedom, which enable them to operate even if one or more phases are lost. This inherent reliability distinguishes them from conventional three-phase motor drives [61]. Open-phase operation in a permanent-magnet synchronous motor refers to a scenario in which one of the

phases of the motor is disconnected or malfunctioning. This situation can lead to an imbalance of magnetic forces and torque, potentially causing the motor to run erratically or stall.
One of promising candidate for such applications is a machine equipped with a dual three-phase winding. This configuration involves two separate windings, each powered by its own converter with half the total power. This machine effectively functions as a six-phase machine under normal operating conditions, yielding enhanced performance.
In the event of a fault, the faulty winding is disconnected, and the machine continues to operate using only the healthy winding.[11].
Several studies documented in the literature explore different topologies, modeling and design methods, and control techniques for multi-phase machines.

3.1 How many phases

As asserted initially, several benefits can be obtained by dividing the stator winding of an electrical machine into more than three phases: functional benefits, inherent in inverter power segmentation, reliability, efficiency, etc.., and in high power, structural and constructive benefits.
Functional benefits result from the configuration of the coils in the stator, how they are arranged and how they are connected.
It is worth mentioning the split-phase configuration, also called asymmetrical, which results from splitting the winding into N three-phase sets displaced by 60/N degree.
The n stator phases can be distributed uniformly over each pole span, instead of being grouped into three-phase set. This stator configuration is therefore known as “symmetrical” n-phase configuration, where n is not necessarily required to be a multiple of three.[15],[49].
The two configurations for creating a nine-phase winding are given as the first example, which will be discussed in more detail later. One choice is to wind each pole group with three three-phase groups and then split each of the three-phase

groups at a single pole into three individual phases, resulting in three separate three-phase windings, shifted by 20 electrical degrees (60/3), as in *figure* 13a. Thus, the second method is to use the symmetrical configuration, is to space the phase groups by 40 electrical degrees (*figure* 13b), to obtain a nine-phase distribution in the magnetomotive force field in air.[49]

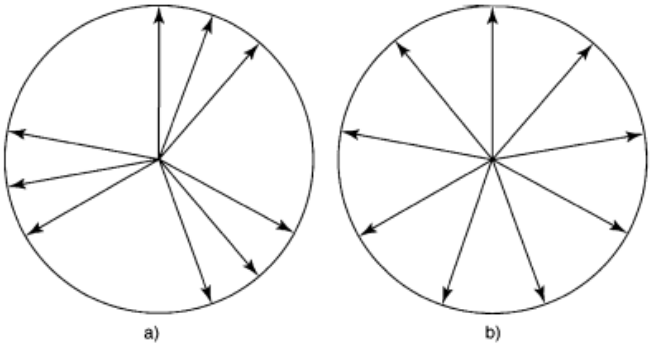

Figure 13: (a) Three separate three-phase windings displaced by 20 electrical degrees. (b) Nine-phase, 40 electrical degree winding distribution. [49]

Another configuration is given by the so called high-power multi-phase machine windings with a "hybrid" winding composition, which results from combining split-phase and symmetrical schemes. In [50] is presented the case of the 15-phase induction machine, where three 5-phase symmetrical phase sets are used, each supplied by a 5-phase inverter. [15].

Figure 14 shows the 15-phase induction machine supplied by 15 IGBT H bridges. As it is said before, the 15 H-bridges are split up into three groups where each group is fed by one dc link.[51].

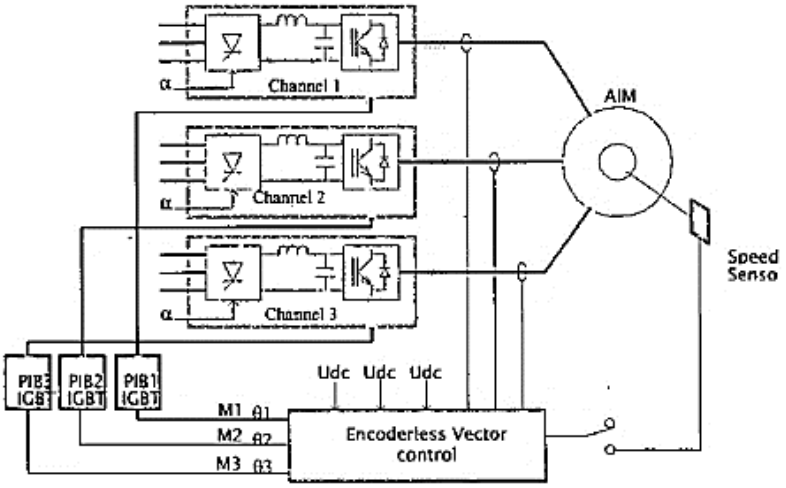

Figure 14:Multiphase machine drive [51]

It is appropriate to proceed with a survey of the multiphase PMSMs most discussed in the literature and found today in commonly used applications such as electric vehicles or residential appliances (e.g., the washing machine) [54], distinguishing their number of phases and arrangement in the stator.

3.1.1 Five phase PMSM

The five-phase permanent magnet synchronous (FP-PMSM) motor has many advantages such as small size, strong fault tolerance, low voltage, and high power.[58].

In contrast to conventional three-phase PMSMs, multiphase PMSMs exhibit distinctive features, including electric, magnetic, physical, and thermal isolation between phases, the capability to restrict short-circuit current and tolerate short circuits between turns. To design a fault tolerant multiphase PMSM, some consideration of these characteristics is needed.

Regarding the choice of phase number, ensuring sustained rated power during single-phase failure is fundamental. When the machine's phase number is N, the power of each phase should be designed to be 1/(N-1) times the rated power: for a five-phase scheme, each phase's overrated power is set at 25% above the normal rating.

In the context of multi-phase speed control systems, common faults involve damage to inverter power devices and open circuits in the motor stator winding, leading to open circuits in one or more stator windings of the motor. Hence, different windings configurations can be exploited to handle such faults.

In general, two different groups of fault tolerant drive systems can be distinguished: topologies, which utilize multiple three-phase drive system working parallel (Y-topologies), and drive systems consisting of electrically separated winding systems, fed from full bridge converters (H-topologies, *Figure 15*).[99]

In H-topology each phase of the motor receives power independently from its dedicated H-inverter bridge and the multi-phase permanent magnet motor can operate with an open phase in the event of a sudden failure, enhancing the motor's control freedom.

In comparison to the conventional Y-connected inverter, the H-bridge inverter offers several advantages: individual and flexible control of each phase, lower voltage stress on the power device due to each H-bridge outputting a phase voltage, robust fault-tolerant performance wherein a failure in one phase or inverter unit does not impact other units, and an increased output level state with minimal output voltage harmonic.[53]

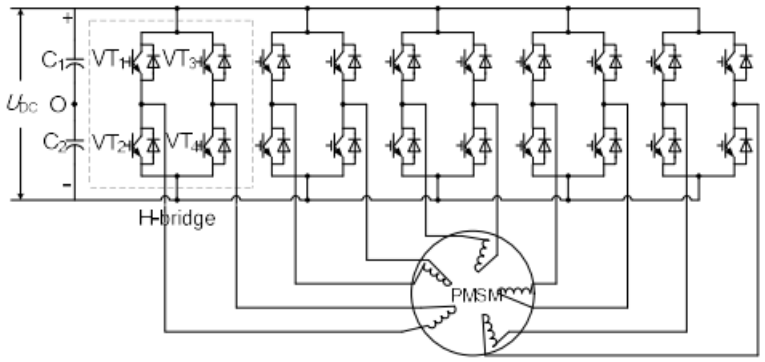

Figure 15: Main circuit of the five-phase H-bridge inverter carried with PMSM [53]

In addition to these advantages, a key point of interest for electric vehicle operation lies in the ability to reduce thermal stress on semiconductors during

standstill or low-speed operation. Another benefit related to the inverter is the lowered current rating for each switch, facilitating the implementation of cost-effective solutions based on discrete semiconductors and PCB-based layouts [98].

The choice of the slot/pole combination must also be taken into consideration (theoretically, the number of the stator slots is integer times of five). [55].

Due to the symmetry of the winding space structure, the five-phase stator winding adopts the star shape connection method [52]. Phase a,b,c,d,e are shifted by 72°. [54]. The mathematical model for the five-phase motor will be constructed, defining equations for voltage, flux, and torque in the rotating reference frame. This process includes the decoupling of torque-producing and flux-producing current components through the d-q transformation.[54],[60].

The stator voltage equation is given by:

$$v_s = \frac{d\lambda_s}{dt} + R_s i_s \tag{3.1}$$

Where R_s, i_s and λ_s are the stator resistance, current and flux linkages matrices, respectively.

Including the effect of third harmonic, a dq transformation can be applied, where the d_1 -q_1 coordinate is rotating at synchronous speed and the d_3 - q_3 coordinate is rotating at three times the synchronous speed [20] (*figure 15*).

$$T(\theta_e) = \frac{2}{5}\begin{bmatrix} \sin\theta_e & \sin\left(\theta_e - \frac{2}{5}\pi\right) & \sin\left(\theta_e - \frac{4}{5}\pi\right) & \sin\left(\theta_e + \frac{4}{5}\pi\right) & \sin\left(\theta_e + \frac{2}{5}\pi\right) \\ \cos\theta_e & \cos\left(\theta_e - \frac{2}{5}\pi\right) & \cos\left(\theta_e - \frac{4}{5}\pi\right) & \cos\left(\theta_e + \frac{4}{5}\pi\right) & \cos\left(\theta_e + \frac{2}{5}\pi\right) \\ \sin 3\theta_e & \sin 3\left(\theta_e - \frac{2}{5}\pi\right) & \sin 3\left(\theta_e - \frac{4}{5}\pi\right) & \sin 3\left(\theta_e + \frac{4}{5}\pi\right) & \sin 3\left(\theta_e + \frac{2}{5}\pi\right) \\ \cos 3\theta_e & \cos 3\left(\theta_e - \frac{2}{5}\pi\right) & \cos 3\left(\theta_e - \frac{4}{5}\pi\right) & \cos 3\left(\theta_e + \frac{4}{5}\pi\right) & \cos 3\left(\theta_e + \frac{2}{5}\pi\right) \\ 1/\sqrt{2} & 1/\sqrt{2} & 1/\sqrt{2} & 1/\sqrt{2} & 1/\sqrt{2} \end{bmatrix} \tag{3.2}$$

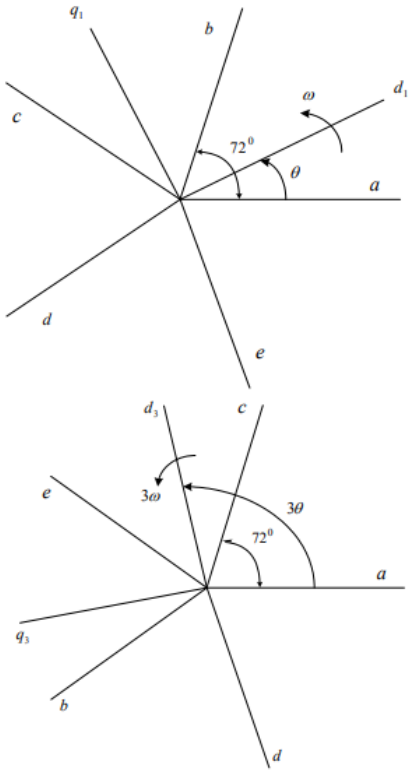

Figure 16: d1 -q1 and d3 -q3 space [60]

The current expression of each phase of the stator winding is as the following:

$$\begin{cases} i_a = I_m \cos(\omega t) \\ i_b = I_m \cos\left(\omega t - \frac{2\pi}{5}\right) e^{j\frac{2\pi}{5}} \\ i_c = I_m \cos\left(\omega t - \frac{4\pi}{5}\right) e^{j\frac{4\pi}{5}} \\ i_d = I_m \cos\left(\omega t - \frac{6\pi}{5}\right) e^{j\frac{6\pi}{5}} \\ i_e = I_m \cos\left(\omega t - \frac{8\pi}{5}\right) e^{j\frac{8\pi}{5}} \end{cases} \quad (3.3)$$

Where I_m is the stator phase current amplitude.

The motor stator current composite vector is expressed as:

$$I = i_a + i_b + i_c + i_d + i_e = \frac{5}{2} I_m(\cos \omega t + j \sin \omega t)$$

(3. 4)

In stable operation, the magnetomotive force space vector formed by the five-phase winding currents can be equivalent to a rotating composite vector whose amplitude is 2.5 times of the phase current.[53]

By applying the above transformation *(3.2)* to the stator voltages and flux linkages equations and calculating the torque become:

$$v_{d1} = L_{d1} \frac{di_{d1}}{dt} + Ri_{d1} - L_{q1} \omega i_{q1}$$

(3. 5)

$$v_{q1} = L_{q1} \frac{di_{q1}}{dt} + Ri_{q1} + L_{q1} \omega i_{q1} + \lambda_{p1} \omega$$

(3. 6)

$$v_{d3} = L_{d3} \frac{di_{d3}}{dt} + Ri_{d3} - 3L_{q3} \omega i_{q3}$$

(3. 7)

$$v_{q3} = L_{q3} \frac{di_{q3}}{dt} + Ri_{q3} + 3L_{q1} \omega i_{q1} + 3\lambda_{p3} \omega$$

(3. 8)

Where λ_{p1} and λ_{p3} are the amplitude of fundamental and third harmonic components of magnet flux linkage [56].

Considering there is saliency on the rotor, the electromagnetic torque is obtained:

$$T_e = \frac{5}{4} p[\lambda_{p1} i_{q1} + 3\lambda_{p3} i_{q3} + (L_{d1} - L_{q1}) i_{d1} i_{q1} + 3(L_{d3} - L_{q3}) i_{d3} i_{q3} + 2L_{m13}(i_{d1} i_{q3} - i_{q1} i_{d3})$$

(3. 9)

The improvement in the developed torque due to the third harmonic can be

noticed from 3.9 [56].

Open-circuit fault condition in a standard star-connected five phase machine is illustrated in *Figure 17* for single-phase (1-Ph) and double-phase faults, namely, adjacent double-phase (A2Ph) fault and nonadjacent double-phase (NA2Ph) fault.

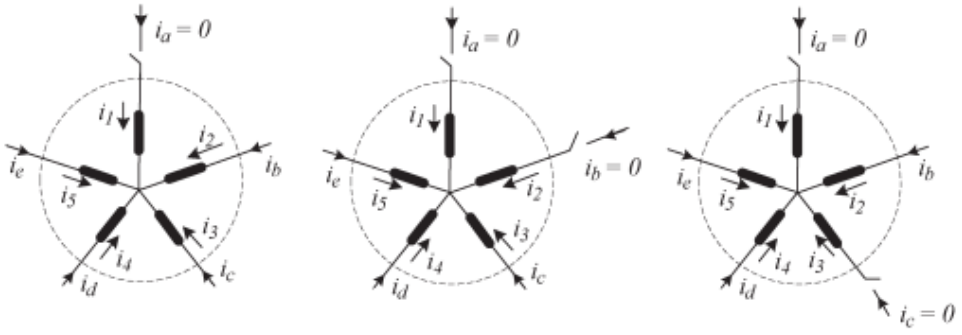

Figure 17:Open-circuit fault conditions of a star-connected five-phase machine from left to right: 1Ph fault, A2Ph fault, and NA2Ph fault [95]

In the event of a missing motor phase, the symmetry of the stator current vector in space is disrupted. This asymmetry leads to torque ripple, consequently it is necessary to reconstruct the phase current to maintain torque constant. To minimize copper loss and maintain the airgap magnetomotive force, adjustments are made to compensate for the stator current of the missing phase. Constraints include keeping the stator flux linkage constant and equalizing the current amplitudes of each phase.

However, the motor system's five stator windings exhibit electromagnetic coupling, making any imbalance in excitation current impactful. Assuming phase A is in fault, adjustments in the residual phase current amplitude and phase are made to align the synthetic magnetomotive force with normal

conditions. Analyzing the decoupling transformation matrix reveals that iq1 and iq3 remain unaffected, while id1, id3, and the 0 axes are influenced by the absence of phase a. [52],[53].

$$\begin{cases} i_b = -i_d = \dfrac{5I_m}{4\,sin^2(\frac{2\pi}{5})}\cos\left(\omega t - \dfrac{\pi}{5}\right) = 1.38I_m\cos\left(\omega t - \dfrac{\pi}{5}\right) \\ i_c = -i_e = \dfrac{5I_m}{4\,sin^2(\frac{2\pi}{5})}\cos\left(\omega t - \dfrac{4\pi}{5}\right) = 1.38I_m\cos\left(\omega t - \dfrac{4\pi}{5}\right) \end{cases}$$

(3. 10)

As it can be seen in (*3.10*) residual four-phase current needs to be increased to 1.38 times of the rated value in order to maintain the rotating magneto motive force before the fault and output the rated torque. After phase a is open-circuited, the space vector diagram corresponding to the remaining 4-phase current is as shown in the *figure 18*.

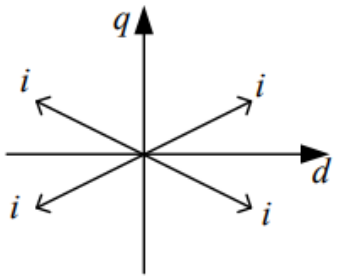

Figure 18: phase diagram of phase currents with phase an open fault [53]

Thanks to the intrinsic characteristics of the motor, number and arrangement of phases and by using the right controller (for example the so-called “vector control” that is easily applicable [56]) to set the current constraints, it is possible to reduce the torque ripple caused by the stator winding open-circuit fault, and

the operation performance of the motor under fault condition can be significantly improved.

Another way to deal with a fault in a single-phase module without leading to a failure of the entire system and, to detect the faulty parts, so that the remaining systems can be used to actively compensate for the influence of a fault, is using smart stator teeth (SST). [94]

A five-phase PMSM with smart stator teeth “SST concept” and without star point connection is presented. The whole power electronics is integrated in the motor housing. Each teeth coil has its own SST module that has gate drivers, a current sensor with analog digital converter, a FPGA and a communication interface inside [91]. This direct connection minimizes space and reduces the number of parts.[94].

A segmented five-phase permanent-magnet synchronous machine is realized as shown in *Figure 19*. The machine includes 10 teeth coil modules in a two-layer winding, 12 loaf-magnets as rotor (*Figure 20*) poles and a distributed inverter with five phase vector control. [92]

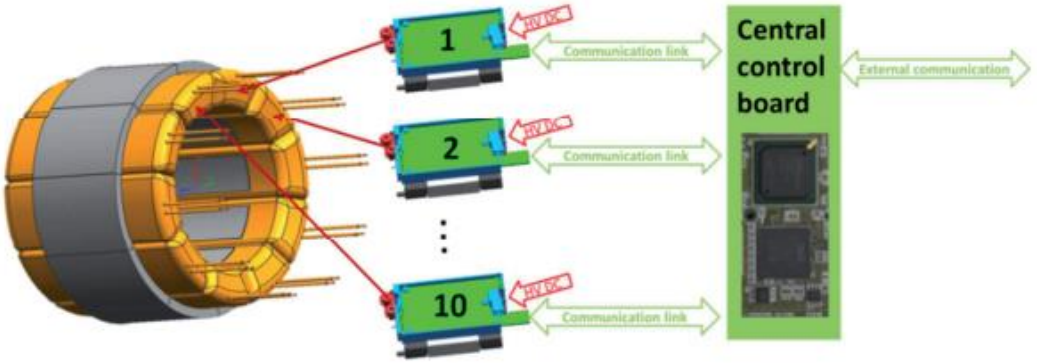

Figure 19:5-phase where teeth coil has its own intelligent full-bridge module [92]

If the stator currents are too high, the permanent magnets are irreversibly demagnetized and for this reason the demagnetization of different magnet shapes must be analyze. The highest demagnetization occurs at the upper corners of the magnet, where the magnet height is smaller. Because of this, shell shaped magnets are favorable for machines with higher overload capacity. [92]

Figure 20: Rotor with shaft [92]

Talking about 5-phase permanent magnet synchronous motors, it is interesting to mention a novel dual stator delta shaped magnet five phase PMSM (NDSDSMFP-PMSM), *figure 21*.
It is used in applications where torque density, robustness and high fault tolerance are required, as in the case of electric vehicles.
Consisting of two stators, double rotor and two sets of 5-phase windings, it is highly suitable for the previously mentioned applications.
Both the rotors have 8 poles embedded in it, which are delta in shape. This configuration allows the magnetic flux to be linked to the internal and external stator so that the magnetic flux density of the two air gaps is increased.

These dual stator models which have two air gaps contribute to the inclusion of the magnetomotive force provided by the inner and outer magnet sets of the rotor. Multiphase, as explained before, increases the torque density and provides high capability for fault tolerance, i.e., it can work continuously even though a few phases are non-operational.[57]

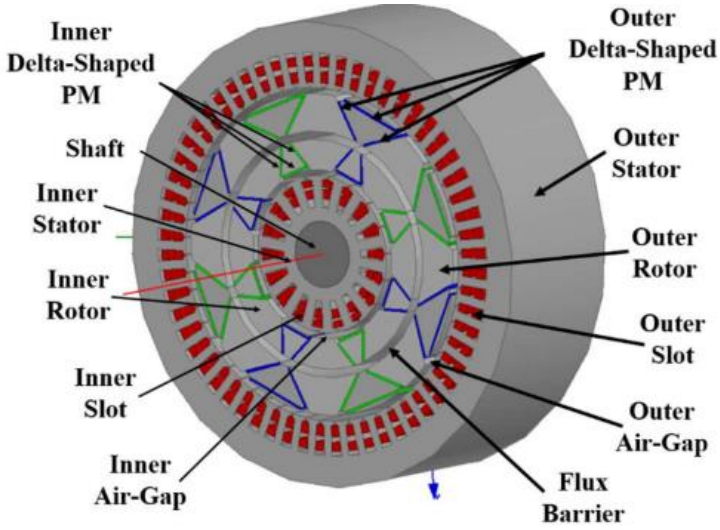

Figure 21: Model of NDSDSMFP-PMSM. [57]

3.1.2 Six phase PMSM

Before reviewing the six phase PMSM, it is useful to point out the difference between two topology of multiphase motors that seem to be the same: dual stator machine and split phase machine.

In this topology, two independent stator windings share the same magnetic structure. However, despite split phase machines, in dual stator machine the two windings may have different number of poles, number of phases or ratings [19].

Among various multiphase solutions, the asymmetric six phase motor is attractive, owing to it intrinsic feature of eliminating 6th harmonic torque pulsation.

The asymmetric six phase PMSM has two sets of three-phase windings.[74]

As previously mentioned, it is also called split-phase.

The phase difference of the windings is 120 electrical degrees in the same three-phase winding unit, while the phase difference between the two groups of three-phase windings can be adjusted according to the practical application.[70]

Two neutrals of windings can be isolated for eliminating the zero-sequence currents [74].

Given the apparent similarities, comparisons between three-phase and six-phase motors are available in the literature, as in [73], where the benefits in loss reduction introduced by using the multiphase motor instead of the three-phase motor were investigated.

The comparison between the two motors is carried out respecting the following constraints:

- the rated current must be the same.
- the 6-phase motor must be obtained only by means of a rearrangement of the windings, halving the number of conductors per slot for each phase; in this way the weights of the two motors are the same.
- the linear current density along the air-gap surface of the stator is kept constant.

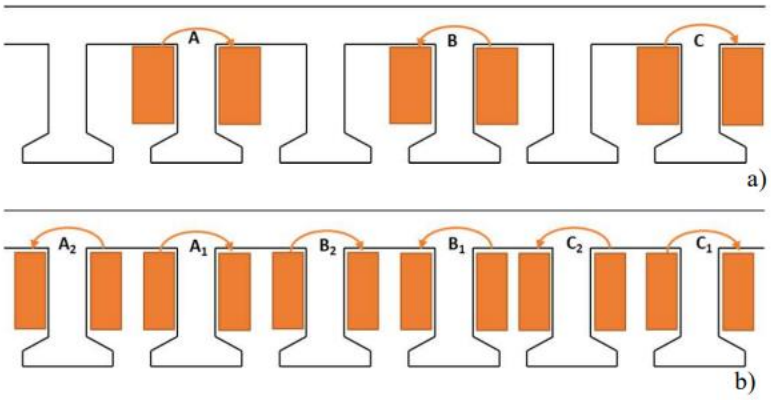

Figure 22:Winding configurations for 24 slots/20 poles: a) 3-ph; b) 6-ph [73]

Having to consider a winding configuration with 24 slots/20 poles for both motors, it is necessary to highlight one more difference, single layer and double layer distribution (*figure 22*).

Single-layer windings have only one phase coil in any slot and do not share the slot with any other phase coils [19].

Double-layer windings coil share a slot, and this results in higher winding inductance compared to a single layer.

Thanks to the arrangement of the coils, single-layer windings are preferred in applications requiring high phase to phase fault tolerance capabilities, instead, the double-layer layout is more suitable for field weakening applications due to lower leakage harmonics.[62]

Through finite element analysis, in [73] an improvement in the electromagnetic torque of the six-phase motor is highlighted, both in terms of ripple and average value, as shown in *figure 23*.

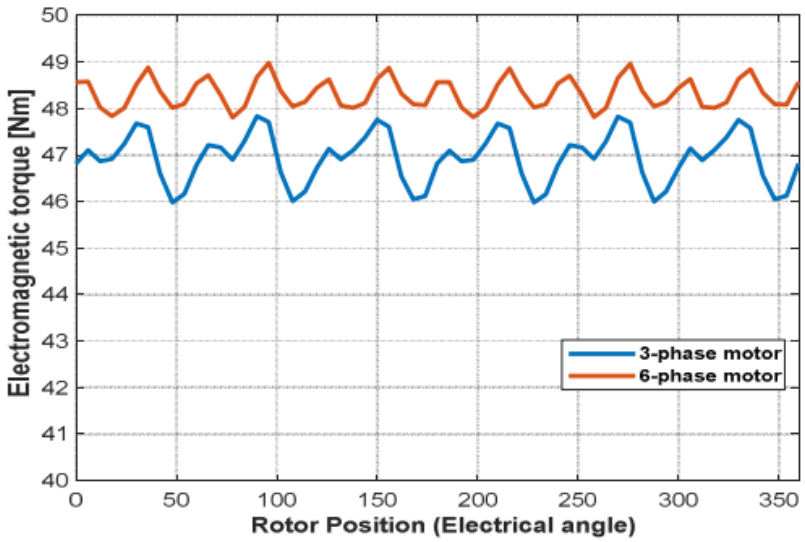

Figure 23: Electromagnetic torque versus rotor position in the steady state rated operating condition [73]

Having already mentioned the multiple d–q frames-based field-oriented control (FOC) scheme where the phase currents in multiple three-phase windings can be controlled separately, and the currents in multiple windings are kept balanced it is now interesting to present another method, that is valid for any multiphase machine type, induction or synchronous, with sinusoidal mmf distribution.[84]

The vector space decomposition (VSD) method is another well-known control scheme for multiphase motor drives, where fundamental components, harmonic components, and zero-sequence components are decomposed onto three kinds of subspaces, namely the torque-component subspace, the harmonic component subspace, and the zero-sequence subspace.[85]

VSD control can provide excellent dynamic torque performance without the influence of coupling voltages between two sets. [75]

The voltage and current space vectors of the asymmetric six-phase PMSM can be decoupled into three two-dimensional orthogonal subspaces: α-β, x-y, and of σ1-σ2. The components on α-β subspace comprise fundamental components related to torque generation. The components on x-y subspace comprise low order harmonic components which do not participate in torque generation. The components on σ1-σ2 subspace are zero-sequence components. [74]

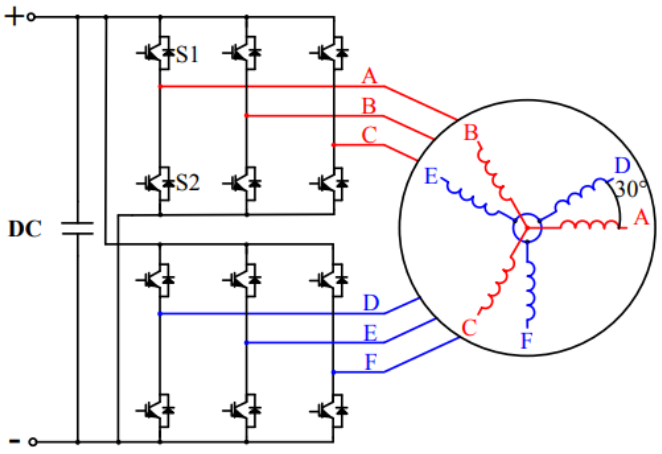

Figure 24:. Configuration of asymmetric six-phase PMSM drive [74]

Considering the configuration in *figure 24*, two-level inverter fed asymmetric six-phase PMSM drives, with separate neutral points. It comes with a drawback; the phase currents contain a substantial amount of extra harmonic content. Decreasing the number of slots per pole per phase leads to a higher harmonic content induced to the stator winding by the rotor field [33].

On the positive side, this configuration allows for the duplication of standard three-phase power electronics hardware, making power supply straightforward without major redesigns. The lower current per semiconductor in this arrangement provides the opportunity to use standard wide band gap semiconductors with typical ratings below 300 A RMS. [32]

It is possible to proceed with the simplification through the decomposition matrix (eq. *3.11*) for VSD:

$$\begin{bmatrix} \alpha \\ \beta \\ x \\ y \\ \sigma_1 \\ \sigma_2 \end{bmatrix} = \begin{bmatrix} 1 & -\frac{1}{2} & -\frac{1}{2} & \frac{\sqrt{3}}{2} & -\frac{\sqrt{3}}{2} & 0 \\ 0 & \frac{\sqrt{3}}{2} & -\frac{\sqrt{3}}{2} & \frac{1}{2} & \frac{1}{2} & -1 \\ 1 & -\frac{1}{2} & -\frac{1}{2} & -\frac{\sqrt{3}}{2} & \frac{\sqrt{3}}{2} & 0 \\ 0 & -\frac{\sqrt{3}}{2} & \frac{\sqrt{3}}{2} & \frac{1}{2} & \frac{1}{2} & -1 \\ 1 & 1 & 1 & 0 & 0 & 0 \\ 0 & 0 & 0 & 1 & 1 & 1 \end{bmatrix} \begin{bmatrix} A \\ B \\ C \\ D \\ E \\ F \end{bmatrix}$$

(3. 11)

After applying the matrix transformation for VSD, a simplified four-dimension equation can be obtained. The corresponding voltage and flux are:

$$\begin{bmatrix} v_d \\ v_q \\ v_x \\ v_y \end{bmatrix} = \begin{bmatrix} R_s & 0 & 0 & 0 \\ 0 & R_s & 0 & 0 \\ 0 & 0 & R_s & 0 \\ 0 & 0 & 0 & R_s \end{bmatrix} \begin{bmatrix} i_d \\ i_q \\ i_x \\ i_y \end{bmatrix} + \frac{d}{dt} \begin{bmatrix} \lambda_d \\ \lambda_q \\ \lambda_x \\ \lambda_y \end{bmatrix} + \omega \begin{bmatrix} -\lambda_q \\ \lambda_d \\ 0 \\ 0 \end{bmatrix} \tag{3.12}$$

$$\begin{bmatrix} \lambda_d \\ \lambda_q \\ \lambda_x \\ \lambda_y \end{bmatrix} = \begin{bmatrix} L_d & 0 & 0 & 0 \\ 0 & L_q & 0 & 0 \\ 0 & 0 & L_{xy} & 0 \\ 0 & 0 & 0 & L_{xy} \end{bmatrix} \begin{bmatrix} i_d \\ i_q \\ i_x \\ i_y \end{bmatrix} + \begin{bmatrix} 1 \\ 0 \\ 0 \\ 0 \end{bmatrix} \lambda_f \tag{3.13}$$

The electromagnetic torque is given by the equation:

$$T_e = 3p(\lambda_d i_d + \lambda_q i_q) \tag{3.14}$$

Since only the components on α-β subspace are related to electromechanical energy conversion, the torque of asymmetric six-phase PMSM can be controlled in similar way as the case of three-phase PMSM.
When the motor phase open occurs, the motor will produce a greater torque ripple that has to be minimized [69].

The theory of alternative current motor winding MMF states that each phase MMF can be split into positive and negative sequence components. When symmetrical currents flow through symmetrical windings, the negative sequence components cancel out. This creates a circular rotating magnetic field using only the positive sequence component. However, in a six-phase double Y-shift 30° winding PMSM with a phase open, torque ripple increases due to not neutralized negative sequence components. To minimize this ripple, it's essential to eliminate the negative sequence synthetic components.
If the two sets of three-phase windings are called: {A1, B1, C1} and {A2, B2, C2}. When the C1 phase winding is open, the remaining five phases still work.
The set of {A2, B2, C2} three-phase windings are still fed with symmetrical currents so there is no negative sequence synthetic component.
Nevertheless, A1 and B1 phases windings produce nonzero negative sequence

components.

Although the position of the remaining phase windings stays fixed (shifted by 120 degree), the controller can determine their time angle.

By appropriately varying the phase angle of the B1 phase winding current, the negative sequence component is reduced to zero.[69]

Selecting the moment of A1 phase current reach the maximum value as the time coordinate zero point, the A1 phase current:

$$i_{A1} = I_m \cos(\omega t) \tag{3.15}$$

so, the current of the B1 phase winding can be expressed as:

$$i_{B1} = I_m \cos(\omega t - x) \tag{3.16}$$

Where I_m is current amplitude, ω is angular frequency.

Therefore, A1, B1 two-phase windings MMFs are:

$$f_{A_1} = F_{\varphi 1} \cos\theta \cos\omega t \tag{3.17}$$

$$f_{B_1} = F_{\varphi 1} \cos(\theta - \frac{2\pi}{3}) \cos(\omega t - x) \tag{3.18}$$

Where $F_{\varphi 1}$ is the fundamental amplitude of MMF

Dividing two MMFs into positive and negative sequence components:

$$f_{A_1} = \frac{1}{2} F_{\varphi 1} \cos(\omega t + \theta) + \frac{1}{2} F_{\varphi 1} \cos(\omega t - \theta) \tag{3.19}$$

$$f_{B_1} = \frac{1}{2} F_{\varphi 1} \cos\left(\omega t + \theta - x - \frac{2\pi}{3}\right) + \frac{1}{2} F_{\varphi 1} \cos\left(\omega t - \theta - x + \frac{2\pi}{3}\right) \tag{3.20}$$

Add f_{A_1} and f_{B_1} to obtain the combined MMF:

$$f = f_{A_1} + f_{B_1} = \frac{1}{2}F_{\varphi 1}\cos(\omega t + \theta) + \frac{1}{2}F_{\varphi 1}\cos(\omega t - \theta)$$
$$+\frac{1}{2}F_{\varphi 1}\cos\left(\omega t + \theta - x - \frac{2\pi}{3}\right) + \frac{1}{2}F_{\varphi 1}\cos\left(\omega t - \theta - x + \frac{2\pi}{3}\right)$$

(3. 21)

where the negative sequence component is:

$$F_{-} = \frac{1}{2}F_{\varphi 1}\cos(\omega t + \theta) + \frac{1}{2}F_{\varphi 1}\cos\left(\omega t + \theta - x + \frac{2\pi}{3}\right)$$

(3. 22)

By reducing the negative sequence component to zero, it can be achieved that the phase angle of the B1 phase winding current needed to decrease the torque ripple when a phase is disconnected. So, the solution is x=60° (*figure 25*).

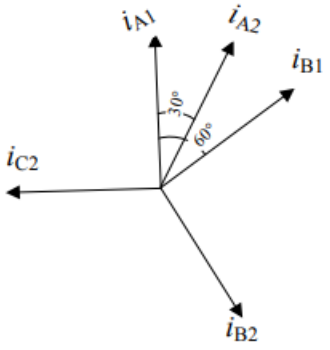

Figure 25: The current phasor diagram after C1 phase open [69]

If on one hand multiphase solutions allow higher fault tolerance, on the other hand they require higher complexity for the inverter, because the number of devices and legs of the inverter depends on the number of phases.[71]

This topic will be discussed later.

In terms of flux-linkages $[\psi]$ and currents *[i]*, the dq-axis can be applied where *[T]* is the transform matrix [38]:

$$\left[\psi_{abc}\right] = [L_{abc}][i_{abc}] \tag{3.23}$$

$$\left[i_{dq0}\right] = [T][i_{abc}] \tag{3.24}$$

$$\left[\psi_{dq0}\right] = [T]\left[\psi_{abc}\right] = \left[L_{dq0}\right]\left[i_{dq0}\right] \tag{3.25}$$

Where inductance matrix is a square matrix of order 6 × 6, partitioned between the two sets of phases, that must consider the mutual coupling between the $a_1b_1c_1$ windings and the $a_2b_2c_2$ windings:

$$\begin{bmatrix} L_{a1} & M_{a1b1} & M_{a1C1} & M_{a1a1} & M_{a1b2} & M_{a1c2} \\ M_{b1a1} & L_{b1} & M_{b1c1} & M_{b1a2} & M_{b1b2} & M_{b1c2} \\ M_{c1a1} & M_{b1c1} & L_{c1} & M_{c1a2} & M_{c1b2} & M_{c1c2} \\ M_{a1a1} & M_{b1a2} & M_{c1a2} & L_{a2} & M_{a2b2} & M_{a2c2} \\ M_{a1b2} & M_{b1b2} & M_{c1b2} & M_{b2a1} & L_{b2} & M_{b2c2} \\ M_{a1c2} & M_{b1c2} & M_{c1c2} & M_{c2a2} & M_{c2b2} & L_{c2} \end{bmatrix} \tag{3.26}$$

The electromagnetic torque can be computed for each set of winding:

$$T_{e1} = 3p\left[\psi_{M1}i_{q1} + \left(L_{d1} - L_{q1}\right)i_{d1}i_{q1} + M_{d1}M_{d2}i_{d2}i_{q1} - M_{q1}M_{q2}i_{d1}i_{q2}\right] \tag{3.27}$$

$$T_{e2} = 3p\left[\psi_{M2}i_{q2} + \left(L_{d2} - L_{q2}\right)i_{d2}i_{q2} + M_{d2}M_{d1}i_{d1}i_{q2} - M_{q2}M_{q1}i_{d2}i_{q1}\right] \tag{3.28}$$

We compare in *figure 26* the two fault tolerant drive topologies, on the left the Y-topology in the case of a 6-phase motor, and on the right the H-topology in

the case of a symmetrical 5-phase motor, as discussed in the previous section,

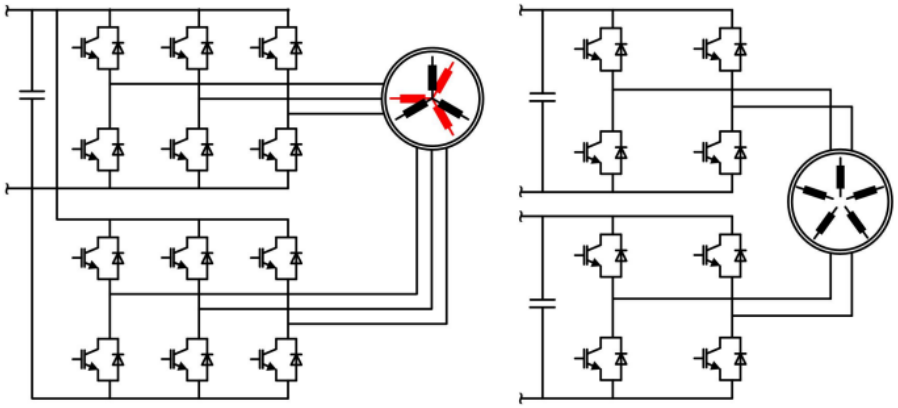

Figure 26:. Fault tolerant drive topologies: Y-topologies (left) and H-topologies (right) [99]

Even in the case of six-phase motors, it is presented in [68], Dual Stator Dual Rotor Six-Phase I-Shaped Permanent Magnet Synchronous Motor (DSDRSPIS-PMSM), *figure 27*, used mostly in electric vehicles due to its efficiency and high performance.

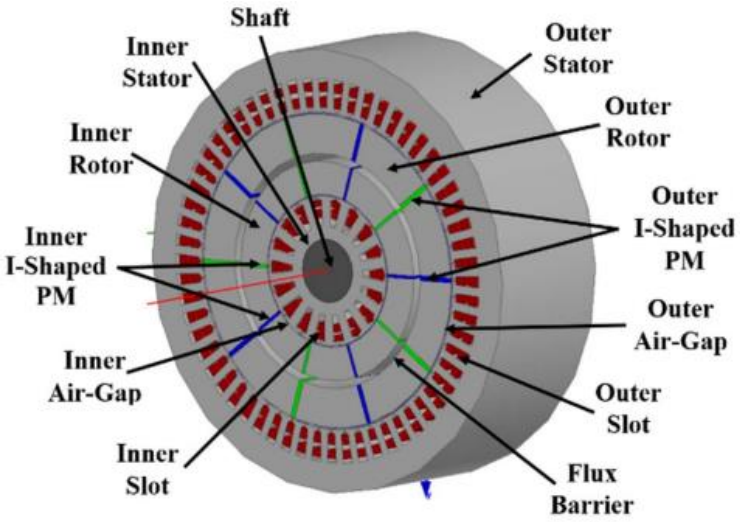

Figure 27: DSDRSPIS-PMSM [68]

3.1.3 Nine phase PMSM

As previously stated, there are two common methods for creating a nine-phase winding.

One choice is to wind each pole group with three, three-phase groups and then split each of the three-phase groups in a single pole into three individual phases *figure 13b*.

One of the advantages of this configuration is that when an open-circuited fault occurs, the whole set of symmetric multi-phase windings containing the fault phase can be cut out of operation [79], *figure 28*.

According to [80], for example, also the twelve-phase PMSM composed of four sets of three-phase windings with the fault phase can operate reliably by neglecting the whole fault symmetrical winding.

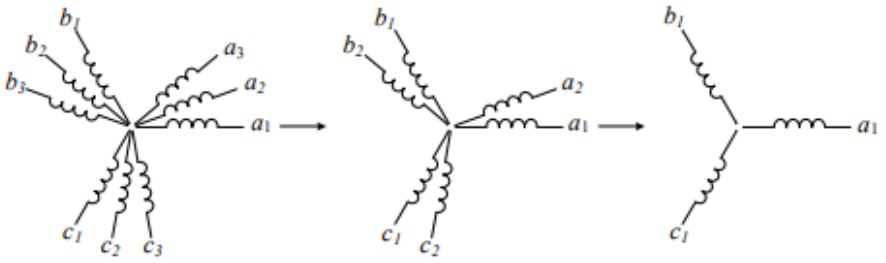

Figure 28: Winding changes in symmetrical fault derating operation [78]

The second choice is to space the phase groups by 40 electrical degrees so that a nine-phase distribution exists in the airgap MMF field [49], *figure 13b*. This results in a symmetric configuration.

Knowing that the development of the control algorithms requires working with the model of the motor, we proceed to model the motor by means of the Park transformation, passing to dq coordinates.

Specifically, considering the split phase configuration (*figure 29*), a first

substantial difference with the three-phase motor emerges: the mutual inductance between the three subsystems windings (which will vary the linkage flux) [76].

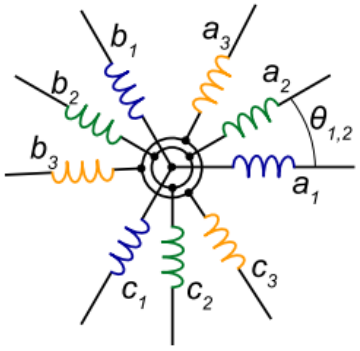

Figure 29: split phase configuration of nine-phase winding [76]

The j-th subsystem can be described as:

$$v_{d_j} = R_j i_{d_j} + \frac{d\lambda_{d_j}}{dt} - \omega\lambda_{q_j} \tag{3.29}$$

$$v_{q_j} = R_j i_{q_j} + \frac{d\lambda_{q_j}}{dt} + \omega\lambda_{d_j} \tag{3.30}$$

Where j={1,2,3} and

$$\lambda_{d_j} = L_{d1} i_{d1} + M_{d1d2} i_{d2} + M_{d1d3} i_{d3} + \psi_{Md1} \tag{3.31}$$

$$\lambda_{q_j} = L_{q1} i_{q1} + M_{q1q2} i_{q2} + M_{q1q3} i_{q3} \tag{3.32}$$

ψ_M permanent magnet flux linkage.

Considering all subsystems with the same electrical characteristic and mutual

inductances:

$$\begin{cases} v_{d_1} = Ri_{d_1} + L_d \dfrac{di_{d_1}}{dt} + M_d \dfrac{di_{d_2}}{dt} + M_d \dfrac{di_{d_3}}{dt} - \omega(L_q i_{q_1} + M_q i_{q_2} + M_q i_{q_3}) \\ v_{d_2} = Ri_{d_1} + M_d \dfrac{di_{d_1}}{dt} + L_d \dfrac{di_{d_2}}{dt} + M_d \dfrac{di_{d_3}}{dt} - \omega(L_q i_{q_2} + M_q i_{q_1} + M_q i_{q_3}) \\ v_{d_3} = Ri_{d_1} + M_d \dfrac{di_{d_1}}{dt} + M_d \dfrac{di_{d_2}}{dt} + L_d \dfrac{di_{d_3}}{dt} - \omega(M_q i_{q_1} + M_q i_{q_2} + L_q i_{q_3}) \end{cases}$$

(3. 33)

$$\begin{cases} v_{q_1} = Ri_{q_1} + L_q \dfrac{di_{q_1}}{dt} + M_q \dfrac{di_{q_2}}{dt} + M_q \dfrac{di_{q_3}}{dt} - \omega\left(L_d i_{d_1} + M_d i_{d_2} + M_d i_{q_3} + \psi_M\right) \\ v_{q_2} = Ri_{q_1} + M_q \dfrac{di_{q_1}}{dt} + L_q \dfrac{di_{q_2}}{dt} + M_q \dfrac{di_{q_3}}{dt} - \omega(M_d i_{d_1} + L_d i_{d_2} + M_d i_{q_3} + \psi_M) \\ v_{q_3} = Ri_{q_1} + M_q \dfrac{di_{q_1}}{dt} + M_q \dfrac{di_{q_2}}{dt} + L_q \dfrac{di_{q_3}}{dt} - \omega(M_d i_{d_1} + M_d i_{d_2} + L_d i_{q_3} + \psi_M) \end{cases}$$

(3. 34)

Torque calculation of triple 3-phase motor is more complicated than a 3-phase PMSM because it must be considered the torque contribution of each subsystem.[76]

$$T_e = \frac{3}{2} p\big[\psi_M\left(i_{q1} + i_{q2} + i_{q3}\right) + \left(i_{d1} i_{q1} + i_{d2} i_{q2} + i_{d3} i_{q3}\right)\left(L_d - L_q\right) + \left(i_{d1} i_{q2} + i_{d2} i_{q1} + i_{d1} i_{q3} + i_{d3} i_{q1} + i_{d2} i_{q3} + i_{d3} i_{q2}\right)\left(M_d - M_q\right)\big]$$

(3. 35)

And the equation of motion is given by [77]:

$$\frac{J}{p}\frac{d}{dt}\omega_r = T_e - T_L - B_m \frac{\omega_r}{p}$$

(3. 36)

Where B_m is the friction coefficient, and J is the rotor shaft inertia.

These sets of equations show how this system is nonlinear, high order and strongly coupling multivariable.

H-bridge inverter circuit is used to drive each phase respectively. The winding

structure of the nine-phase PMSM and the nine-phase H-bridge drives are shown in *figure 30*.[81].

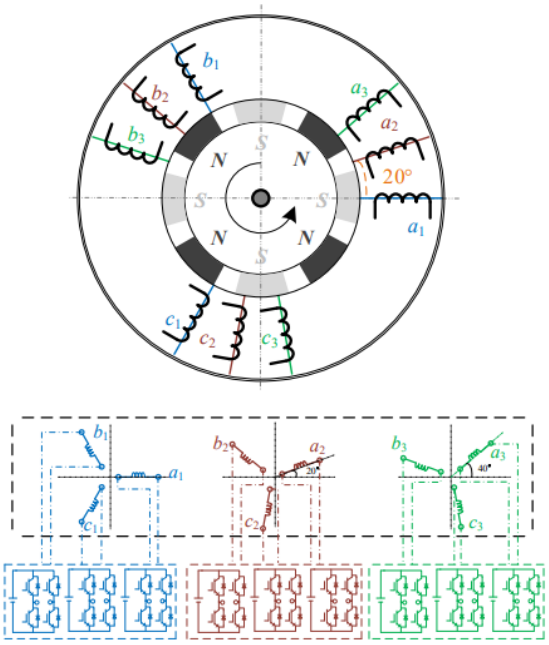

Figure 30: Winding structure and H-bridge drives of Nine-phase PMSM [81]

Another option is presented in [15], where the winding sets are shifted by 120 electrical degree, *figure 31*.

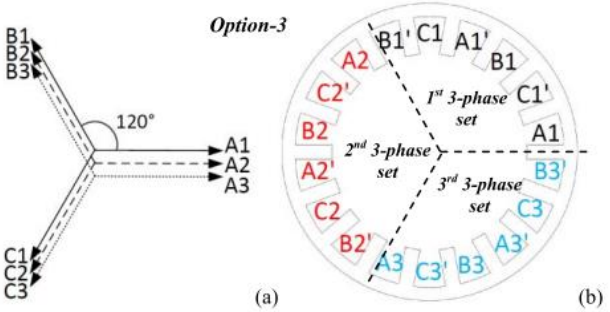

Figure 31: (a) Phasor diagram of nine-phase winding and (b) winding sets [15]

Since the coil length from phase A1 to A1' is the shortest between the option listed, the motor end windings are the smallest and this leads to a lower copper loss.

Chapter 4
Multiphase drive

Repeatedly stated, multi-phase motor drives (MPD) have various advantages over traditional three-phase counterparts. They reduce torque ripple, decrease stator current per phase without increasing voltage, and enhance overall reliability and power density [26]. Addressing a drawback in three-phase inverter operation, the low-frequency torque ripple, increasing the number of phases in the machine emerges as the optimal solution [27].

The first current harmonic generates the fundamental wave of the resulting magnetic field, rotating at synchronous speed. Higher-order current harmonics contribute to additional losses, noise, vibration, torque ripple, and reduced motor performance with non-sinusoidal current. Increasing the number of phases has been proven to mitigate losses in the rotor caused by these current harmonics [20].

Therefore, multi-phase systems offer benefits such as lowering stator current per phase without increasing voltage, reducing dc link current harmonics, improving reliability, and increasing torque per rms ampere for the same volume machine. Enhancements in noise characteristics and a decrease in stator copper loss are additional advantages of multi-phase systems [19].

Multiphase machines are highly used in variable-speed applications, they are employed in ship propulsion, locomotive traction, hybrid electric vehicles, battery chargers. [82]

The origin of multiphase variable speed drives can be traced back to the late 1960s, the time when inverter-fed ac drives were in the initial development stage.[90]

Power electronic converters have become the recent norm for supplying and controlling electrical drives. These converters enable the drives to function across all possible regions, achieving the desired speed and torque [48]. In the case of PMSM, power is drawn from a battery, and converters play a crucial role

in transferring power from the battery to the load (as depicted in *figure 32*), involving the conversion from DC to AC. The DC power obtained is converted into AC using a cascaded H-bridge type multi-level inverter. The PMSM receives the necessary power from the inverter, catering to the load requirements. The multi-level inverter serves two primary functions:

Adjusting the phase, magnitude, and frequency of stator currents to control the speed of the PMSM based on the provided speed reference.

Converting power from DC to AC for supply to the motor [103].

In the converter, the main components contributing to power dissipation are the transistors and DC link capacitors. The modular design ensures that the total power of the drive is distributed among multiple modules, thereby reducing the power per module, and minimizing power losses in both the transistors and DC link capacitors [100].

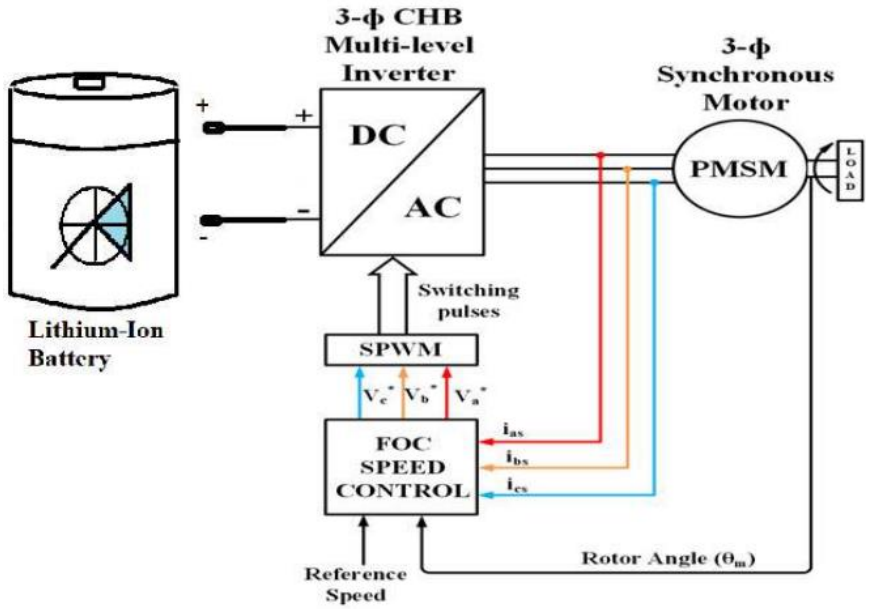

Figure 32: Block diagram of Battery connected multi-level inverter fed PMSM [103]

4.1 DC link

The dc link circuit in an electric motor system serves as an interface between the power source and the motor, enabling efficient power conversion, voltage

regulation, and precise control of motor performance. It plays a central role in the functionality and overall performance of electric motors used in various applications, including electric vehicles, industrial machinery, and household appliances. The main component is the dc link capacitor.

To show an example of interface between power supply and motor, in *figure 33* is shown the cascaded bidirectional DC-DC converter plus voltage source inverter (VSI) topology with a common DC-link capacitor that is one of the most common powertrain topologies in electric drives in EVs and HEVs.[106]

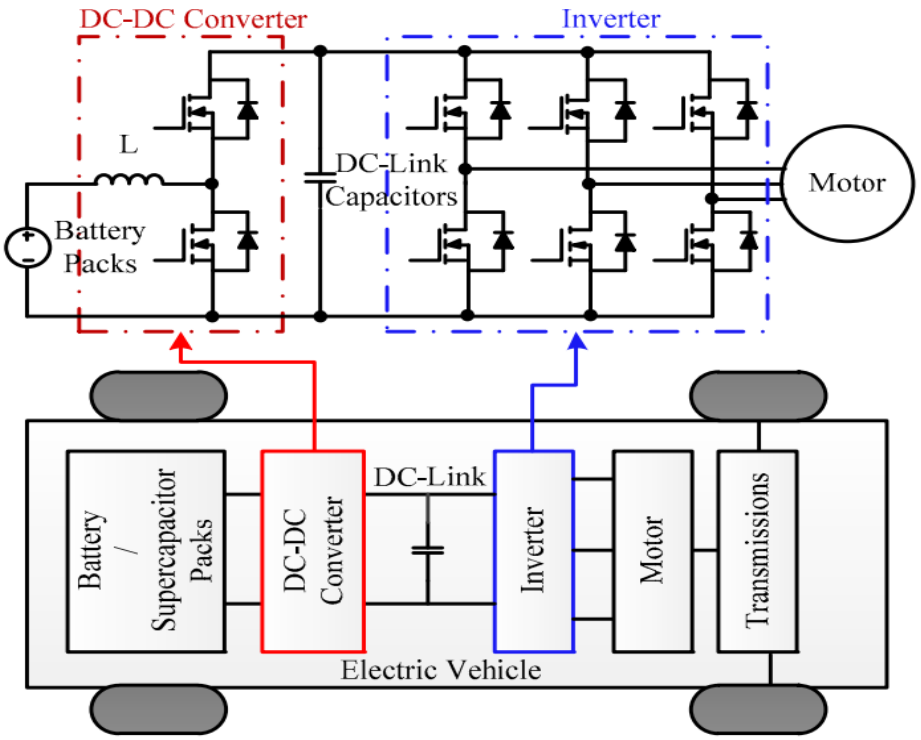

Figure 33:. Electric vehicle with cascaded bidirectional DC-DC converter plus 3-phase voltage source inverter drive system [106]

The DC bus capacitor serves in maintaining a stable DC bus voltage and ensuring smooth battery current in voltage source inverter (VSI)-based traction drive systems employed in electric vehicles (EVs), hybrid EVs (HEVs), and plug-in HEVs (PHEV).

The VSI, composed primarily of six power semiconductor switches, typically

insulated gate bipolar transistors (IGBTs), along with a DC bus filter capacitor, operates by switching the battery's DC voltage to generate a desired set of three-phase AC voltages through a selected pulse width modulation (PWM) scheme. These AC voltages, in turn, regulate motor current to control both torque and speed [101].

Due to its significant impact on volume, weight, and cost, it is crucial to avoid overdesigning the DC-link capacitor. On the other hand, an excessively small capacitance may result in high DC-link voltage ripple, influencing the PWM process and potentially distorting output voltages, even with feedback control. Therefore, an extensive analysis of DC-link current and voltage ripples is crucial for the effective design of the DC-link capacitor [102].

The dc link ripple current is proportional to the magnitude of the phase current. About 20% of the inverter material cost is from the dc link capacitor of which capacity is determined by the ripple current. So, for size and cost reduction of the capacitor, it is important to reduce the ripple current in the dc link [111].

The procedure for sizing the DC link capacitor begins with two basic steps. Initially, the maximum means square ripple current (rms) to be handled by the DC link capacitor is calculated. Next, the frequency spectrum of the current waveform is analyzed. It is important to ensure that the maximum rms ripple current remains below the nominal ripple current of the selected capacitor. This ensures that a suitable capacitor is selected.[100]

Figure 34 shows a flow chart that summarizes the generic design process of a capacitor.

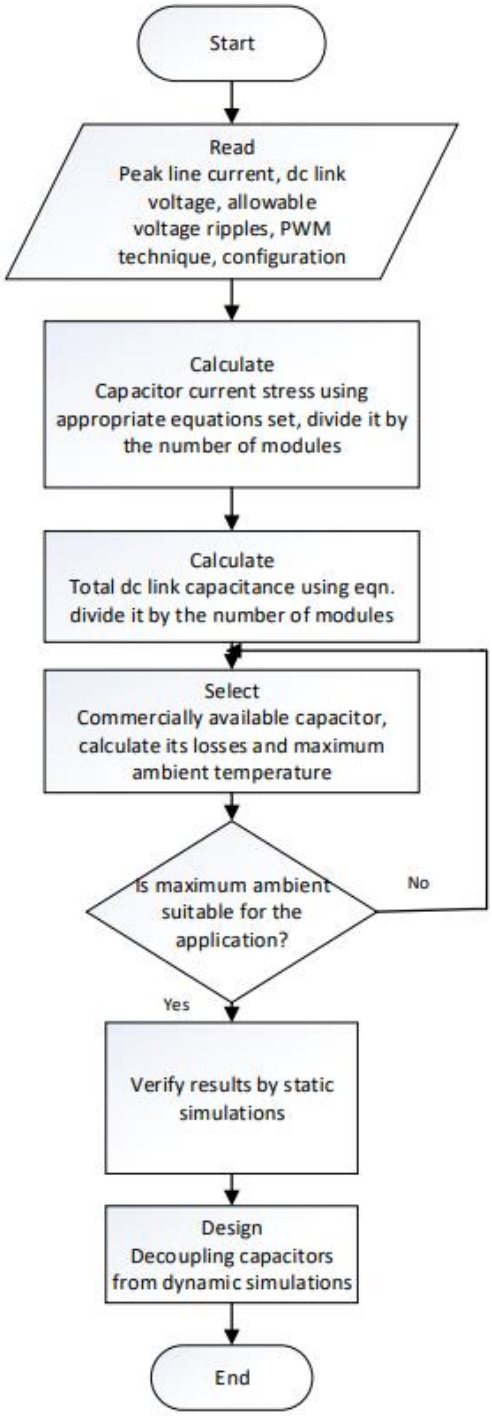

Figure 34:Generic DC link capacitor design flow chart [100]

In [100] an example of capacitor calculation process for the 15-phase PMSM prototype is presented which involves several sequential steps. Beginning with the intersection plotting technique, capacitor peak harmonic current (i_{ch}) is determined using specific parameters such as $i_{linepeak}$, g (number of groups), N (number of phases), Φ (phase shift between output voltage and output current of the inverter), θ (electrical phase shift between phases), and K (interleaving angle).

Then, the calculation proceeds to identify harmonic components, including the rms current (I_{crms}) from the obtained values. Further steps involve determining the most dominant equivalent harmonic (I_{mde}) and establishing the minimum value of dc link capacitance (C_{min}), equation (4.1). The peak dominant harmonic component (I_{chpea}) and its corresponding frequency (f_{md}) are considered, along with the peak-to-peak dc link voltage ripple ($V_{ppripple}$).

$$C_{min} = \frac{I_{mde}}{\pi f_{md} V_{ppripple}} \tag{4.1}$$

To optimize the approach, the total dc link capacitance and current stress are divided among modules, allowing for a modular and efficient system. The current stress and capacitance per module are then computed by dividing the relevant equations by the number of modules. This modular approach facilitates the selection of a commercially suitable capacitor based on specific criteria, including rms current stress, dc link voltage, and dc link capacitance values.

The reduction of the RMS current is necessary to decrease the size of DC link capacitors and alleviate their stress.

Another significant factor is the lifetime of the capacitor. In automotive applications, meeting the 15-year or 241,302 km lifetime requirement is a critical guideline for selecting DC link capacitors. However, as the applied voltage and core temperature increase, the lifetime decreases. To address this, the most effective method, given specific ambient temperature and thermal resistance conditions, is to minimize the capacitor's loss. Thermal loss,

determined by the capacitor current, is the dominant factor in total capacitor loss. Hence, reducing the current in the DC-link capacitor is necessary to extend its lifetime or decrease the required capacitance. [107]

Figure 35 illustrates a comparison of the required capacitance, measured in per unit (p.u.), for different MPDs. The base value is set for the three-phase case, and the graph demonstrates a decrease in required capacitance with an increasing number of phases, reaching its lowest for the twelve-phase system There's a significant reduction in dc-link capacitance when comparing three-phase and five-phase cases. The curve continues to decrease for six-, seven-, and nine-phase drives. However, the capacitance required for nine-, eleven-, and twelve-phase machines appears to stabilize. When transitioning to a six-phase drive, the dc-link capacitor values almost halve, offering potential benefits for converter efficiency.[48]

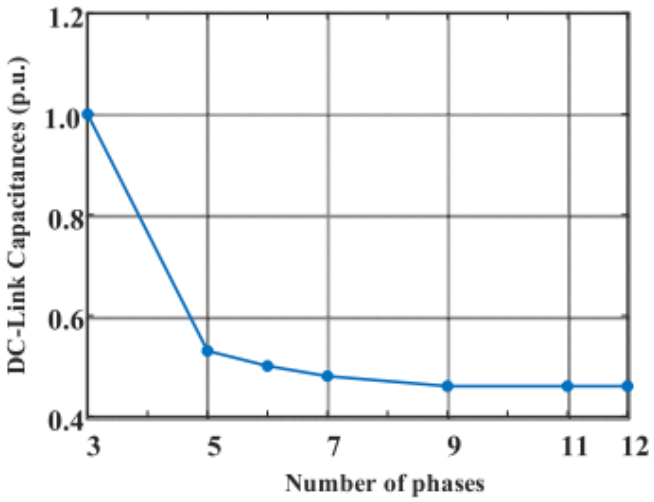

Figure 35: Required dc-link capacitance for different MPDs [48]

Reference [83] illustrates that for the same power output, the magnitude of the phase current is inversely proportional to the inverter phase number, as indicated by the normalized values in Table 2. The RMS current rating of the DC-link capacitor is determined by multiplying the maximum normalized DC-

link RMS current by the phase RMS current. As can be noticed, DC-link capacitor RMS current rating decreases slightly with the increased phase number in VSIs.

Table 2:DC-link capacitor RMS ratings comparison for different phase number [83]

Machine phase number	The maximum normalized DC-link RMS current	Phase current	Per unit DC link RMS rating
3	0.65	1.00	1.00
4	0.81	0.75	0.94
5	0.99	0.60	0.91
6	1.17	0.50	0.90
7	1.36	0.43	0.90
8	1.55	0.38	0.89
9	1.74	0.33	0.89
10	1.93	0.30	0.89
11	2.12	0.27	0.89
12	2.31	0.25	0.89
13	2.50	0.23	0.89
14	2.69	0.21	0.89
15	2.88	0.20	0.88
16	3.07	0.19	0.88
17	3.26	0.18	0.88
18	3.45	0.17	0.88
19	3.64	0.16	0.88
20	3.83	0.15	0.88

Capacitors are generally divided into three types: electrolytic, film, and ceramic capacitors. For VSI DC-link capacitors, choices often include aluminum electrolytic capacitors, metallized polypropylene film capacitors, and high-capacitance multi-layer ceramic capacitors. This preference is due to their high current rating and large capacity per unit volume. However, while aluminum

electrolytic capacitors and metallized polypropylene film capacitors are commonly used, multi-layer ceramic capacitors are less popular in this application due to their higher cost and sensitivity to temperature and terminal voltages, which affect their capacitance.[83]

4.2 Power electronic converters

This section explores the topic of inverters in the context of multiphase machines. Symmetrical and asymmetrical machines have been discussed, based on the arrangement of phases. In a symmetrical machine, a spatial displacement of 360/n electrical degrees exists between the magnetic axes of two consecutive phases. For example, a five-phase machine has a spatial displacement of 72 electrical degrees between consecutive phases. When the number of phases is even or odd and not prime, the machine can be imagined as a set of m, each containing a phase. Typically, a=3 (three-phase sets), m=2,3,4,5..., and the spatial displacement between the first phases of two consecutive sets is 180/n electrical degrees. For example, a six-phase asymmetrical machine consists of m=2 three-phase sets (a=3), with a spatial displacement of 30 electrical degrees between the first phases of the two three-phase sets. Similarly, a twelve-phase asymmetrical machine has m=4 three-phase sets, and the spatial displacement between the first phases of two consecutive sets is 15 electrical degrees. This intricate interplay between symmetry, asymmetry and number of phases sets the stage for an exploration of inverters in multiphase machines.

The most employed drive configurations (machine and inverter) are the following: [105],[88]

1. Conventional multiphase with single machine neutral point (*figure 36*).
2. Multiple of independent single-phase units (*figure 37).*
3. Multiple of independent three-phase units (*figure 38*).

The configuration employing multiple independent three-phase units (refer to figure 38) is suitable when the phase number is a multiple of three, applicable to

both symmetrical and asymmetrical machines. In this setup, the stator comprises independent three-phase windings with isolated neutral points. Each three-phase set is individually powered by a dedicated three-phase inverter. This design allows for the use of three-phase power electronics modules, resulting in a reduction in converter size, cost, and design time. Furthermore, the multiple three-phase approach often simplifies control schemes, as the number of independent currents is lower compared to the multiple single-phase approach.

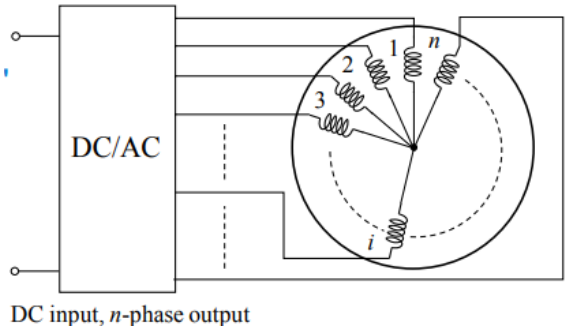

Figure 36: Conventional multiphase topology with single neutral point [105]

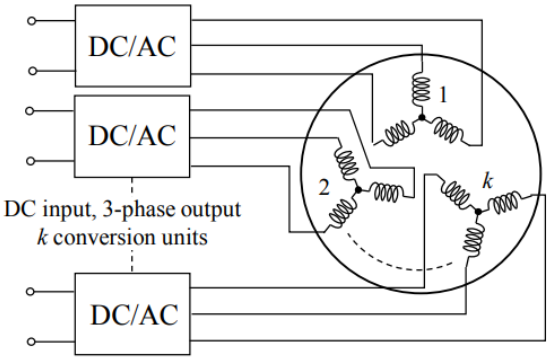

Figure 37: Multiphase topology with multiple single-phase units. [105]

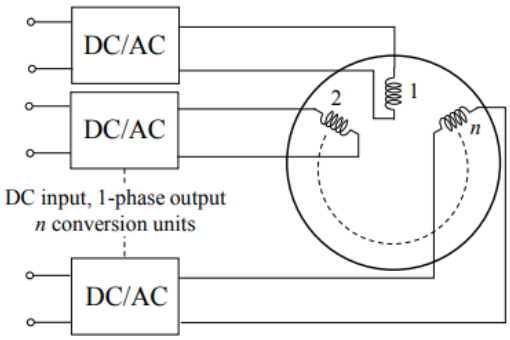

Figure 38: Multiphase topology with multiple three-phase units [105]

In MPDs, power distribution occurs across a greater number of phases, with each phase being fed from a converter leg utilizing a single component rather than parallel components.

The adoption of MPDs effectively resolves issues associated with parallel device configurations, even if at the cost of increased assembly complexity due to the growing number of wires.

Illustrated in figure 39 is the reduction in phase current for various multiphase machines, specifically, those featuring five, six, seven, nine, eleven, and twelve phases. As in case of DC capacitor in previous section, all phase currents are expressed in per unit values, with the three-phase case's phase current serving as the base value.

The relationship between the number of phases and per-phase current is inversely proportional. The five, six, and seven-phase scenarios exhibit a substantial decrease in per-phase currents compared to the three-phase case.

This, in turn, facilitates the use of semiconductor switches with lower ratings.[27]

As the number of phases increases, the reduction in per-phase current becomes less marked, as seen in the transition from the eleven-phase to the twelve-phase case. Six-phase machines, for instance, show phase currents that are exactly half of those observed in three-phase machines.

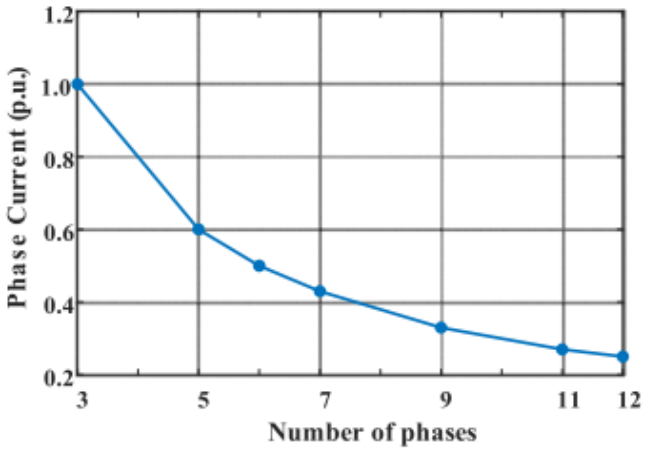

Figure 39: Phase currents in p.u. for different MPDs [48]

Instead of parallel operation to control a single phase, these modules can be independently controlled to manage distinct phases, presenting a strategic advantage in design flexibility and module utilization.[48]

Taking the example of a nine-step system. It necessitates three times more power contacts, each carrying approximately a third of the current. Additionally, in a perfectly modular nine-phase system, the number of sensors for variables like temperature or DC-link voltage increases by a factor of three, with the option to use additional sensors for redundancy. The size of discharge resistors scales with the capacity of the DC-link, and in a modular nine-phase system with reduced total capacitance, three separate discharge devices are needed instead of a single device, each capable of handling less than a third of the power. The half bridge driver in a nine-phase system should deliver, for the same number of total chips, approximately one third of the output power, which helps in downsizing the power supply, the output stage, and the gate resistors. To minimize the impact on the total volume and total cost of the increasing driver effort, integration of the analog and digital logics as well as of the insulation devices in Application Specific Integrated Circuits (ASIC) can be pursued.[25]

The dc-link voltage can be reduced to where N is the number of segments per phase and $V_{dc,3W}$ is the dc-link voltage required by the original three-wire inverter.

$$V_{dc} = \frac{V_{dc,3w}}{N}$$

(4. 2)

Another benefit of the multiphase converter is distributed power dissipation. In the conventional sixpack power module for the three-phase inverter, power losses are concentrated, while for the multiphase converter the losses are distributed in N H-bridge power module and loss for each module is also much smaller. This provides great advantage for the thermal design of high-power electronically controlled motor (ECM). The multiphase converter also provides lower electromagnetic interference (EMI). Each H-bridge converter can be placed very close to the segment winding, this significantly reduce the stray inductance and noises coupling of the power circuit. The common mode EMI is also significant reduced due to the much lower dc-link voltage.[63]

4.2.1 Topologies and modulation

There are different topologies used for MPDs, classified into three categories based on the structure and number of levels of their respective output voltage:

A. Two level inverters
B. Dual supply inverters
C. Multilevel inverter

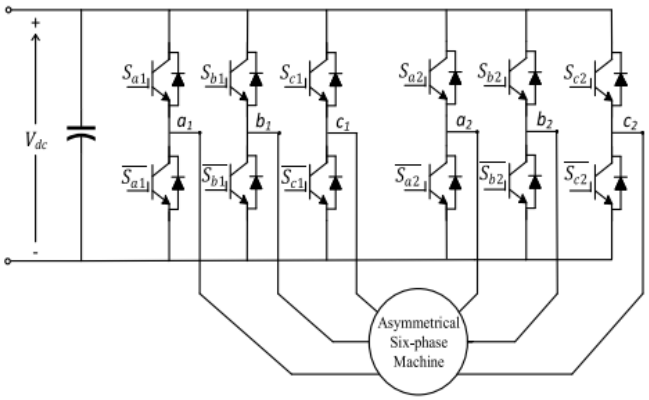

Figure 40: Two-level inverter-fed six-phase machine [48]

A. Two level inverters (*figure 40*) are extensively investigated due to its simple structure and the availability of industrial packs from

manufacturers. Compared to more complex topologies like matrix, multilevel, and open-end converters, it requires only two three-phase bridges and straightforward controllers. Three modulation techniques for operating a six-phase inverter in electric vehicle (EV) applications are presented:

1. Carrier-Based PWM (CPWM):

Utilizes reference signals generated from a control scheme representing two sets of three-phase outputs shifted by 30 degrees. Compares reference signals to a carrier signal, and the output signals are used to control the inverter switches.
Simplicity and reliability make CPWM suitable for EV applications, but it has limitations in control degrees for optimizing converter performance.

2. Double Zero-Sequence Injection (DZSI):

Involves injecting zero-sequence components into reference voltages to lower total harmonic distortion (THD) and extend the linear control region of the inverter. Simpler to implement than vector classification techniques and can improve harmonic profile.

3. Space-Vector PWM (SVPWM) Based on VSD Theory:

Using such transformation enables the control of the full six-phase converter as a single unit. Utilizes various switching states (64 in total) to control a six-phase inverter.
The states are assigned numerical values from 0 to 63 in binary format, considering each upper switch as a digit in the binary representation (S_{c2}, S_{b2}, S_{a2}, S_{c1}, S_{b1}, S_{a1}). In this way, the initial switching state is (000000) and the final state is (111111). By implementing these switching states in the inverter, it is possible to calculate the output phase voltage for both the two isolated neutral (4.3) and the single isolated neutral connections (4.4) [112]:

$$\begin{bmatrix} V_{a1} \\ V_{b1} \\ V_{c1} \\ V_{a2} \\ V_{b2} \\ V_{c2} \end{bmatrix} = \frac{V_{dc}}{3} \begin{bmatrix} 2 & -1 & -1 & 0 & 0 & 0 \\ -1 & 2 & -1 & 0 & 0 & 0 \\ -1 & -1 & 2 & 0 & 0 & 0 \\ 0 & 0 & 0 & 2 & -1 & -1 \\ 0 & 0 & 0 & -1 & 2 & -1 \\ 0 & 0 & 0 & -1 & -1 & 2 \end{bmatrix} \begin{bmatrix} S_{a1} \\ S_{b1} \\ S_{c1} \\ S_{a2} \\ S_{b2} \\ S_{c2} \end{bmatrix}$$

(4. 3)

$$\begin{bmatrix} V_{a1} \\ V_{b1} \\ V_{c1} \\ V_{a2} \\ V_{b2} \\ V_{c2} \end{bmatrix} = \frac{V_{dc}}{6} \begin{bmatrix} 5 & -1 & -1 & -1 & -1 & -1 \\ -1 & 5 & -1 & -1 & -1 & -1 \\ -1 & -1 & 5 & -1 & -1 & -1 \\ -1 & -1 & -1 & 5 & -1 & -1 \\ -1 & -1 & -1 & -1 & 5 & -1 \\ -1 & -1 & -1 & -1 & -1 & 5 \end{bmatrix} \begin{bmatrix} S_{a1} \\ S_{b1} \\ S_{c1} \\ S_{a2} \\ S_{b2} \\ S_{c2} \end{bmatrix}$$

(4. 4)

The transformation matrix (3.11) is utilized to apply a conversion to the resulting output voltages, transferring them into the decoupled sub-planes (V_α–V_β), (V_x–V_y), and (V_{o+}–V_{o-}).

4. Vector Classification Technique (VCT):

Based on double-DQ theory, offering simplicity and enhanced dc-link voltage utilization. Two distinct approaches have been employed to implement this technique. The initial method involves utilizing two references rotating within a familiar hexagon, depicting all conceivable switching vectors of the three-phase inverter. In contrast, the second approach entails rotating one of the hexagons by 30 degrees and employing a single reference.
Comparison with SVPWM methods shows better harmonic minimization with the latter.[48]

The five-leg inverter (*figure 41*) presents an alternative topology with fewer switches compared to the traditional six-phase drive inverter. This configuration involves linking one machine phase to the midpoint of the dc-link, serving as a reference for the other phases. However, a key challenge in employing this topology lies in achieving a balanced midpoint voltage [48].

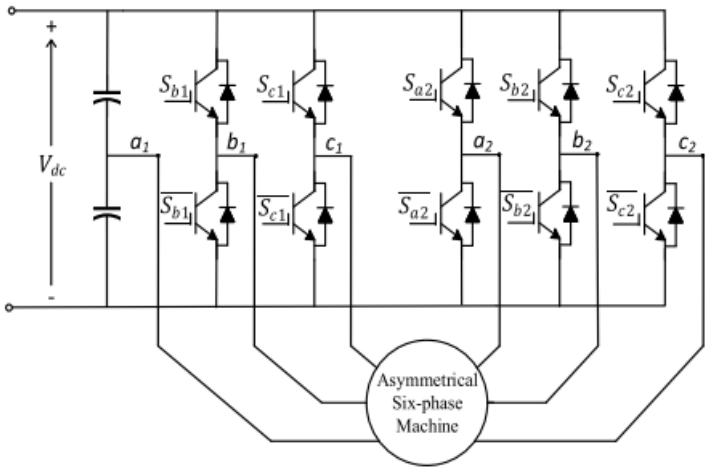

Figure 41:Five-leg inverter topology [48]

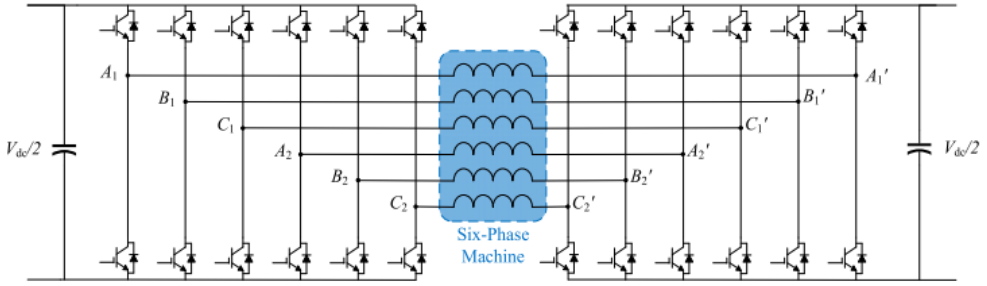

Figure 42: Dual-supply, inverter-fed, open-end, winding six-phase machine I [48]

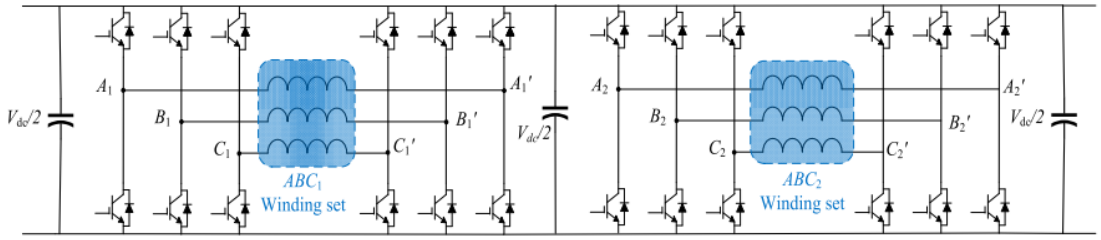

Figure 43:Dual-supply, inverter-fed, open-end, winding six-phase machine III [48]

The dual-supply inverter topology is utilized for machines with an open-end winding configuration and is powered by isolated dc sources, eliminating the need for capacitor voltage balancing. The cascaded H-Bridge multilevel

topology, commonly used in EV applications, also relies on isolated dc sources, often supplied by custom-designed phase-shifting transformers. Various topologies have been introduced based on the supplies used and their connections. The dual-supply topology I (*figure 42*) involves two-sided supplies, each connecting to a converter output from both phase terminals. Another topology, dual supply topology II, utilizes a single supply for two inverters in a five-phase drive, aiming to eliminate common-mode voltage using SVPWM. There was proposed dual supply topology III (*figure 43*), featuring four three-phase inverters with two supplies connected from both sides and a shared capacitor. This topology helps suppress fifth and seventh harmonics in the output voltage, at the expense of an additional capacitor bank. In comparing symmetrical and asymmetrical six-phase drives with an open-end configuration, it is noted that symmetrical drives exhibit similar results to three- and five-phase drives. However, asymmetrical drives demonstrate varied behavior based on the applied modulation techniques, emphasizing the impact of drive configuration on performance.

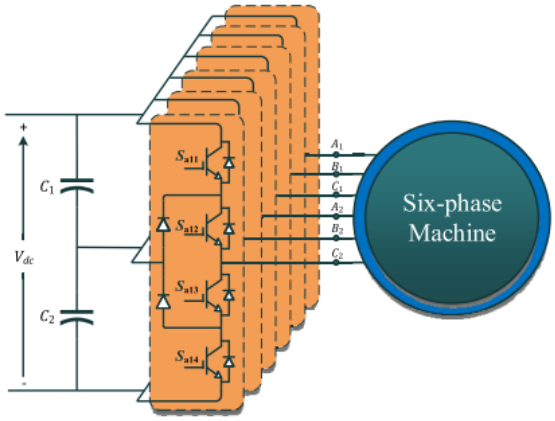

Figure 44:NPC-fed, six-phase machine [48]

Multilevel inverters are widely considered for high-voltage, high-power motor drives, with various topologies evaluated based on factors like cost, size,

performance, and complexity. As the push for higher dc-link voltages (>800V) in the next generation of electric vehicles (EVs) continues, multilevel topologies, particularly the neutral-point clamped inverter (NPC), *figure 44*, emerge as promising candidates for enhancing output power quality and overall efficiency. Like two-level topologies, SVPWM techniques for multilevel multiphase drives are classification-based and Voltage Space Vector Diagram (VSD) based. VSD-based models are also discussed in different literature, it is discussed (in [113]) a method where it is added a decoupling, especially for developing a switching pattern based on VSD. Selecting the optimal switching vector proves to be a challenging, crucial for maintaining a balance in the midpoint of the dc-link and minimizing output circulating currents. Consider the configuration depicted in Figure 45. In this setup, an asymmetrical winding configuration is employed for the PMSM, featuring a 30-degree phase shift between dual three-phase windings. O1 and O2 represent the neutral points of the two windings, and n denotes the midpoint of the DC link. To control NPC-3L dual three-phase PMSM drives, the initial step involves designing VSD-based space vector modulation (SVM). The output voltage for each inverter leg of NPC-3L can be $V_{dc}/2$, 0, $-V_{dc}/2$, and these values are denoted as 2, 1, 0, respectively. Consequently, the NPC-3L dual-three-phase inverter has a total of 3^6 (729) voltage vectors, each represented in decimal form. Given the multitude of voltage vectors, the primary task is to reduce the candidates for practical use. This is achieved by exploiting the relationships among phase voltages in different large sectors. To optimize the drive system's performance, the selection of these five voltage vectors aims to synthesize the desired voltage reference on the $\alpha - \beta$ plane, minimize harmonics on the $x - y$ plane, and simultaneously incorporate redundant voltage vectors for controlling voltage at the midpoint of the DC link. [113]

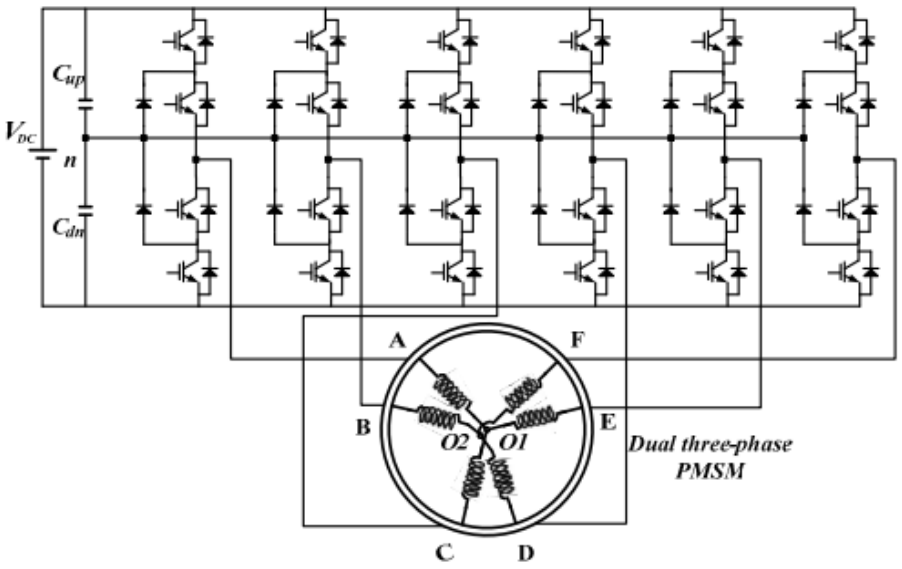

Figure 45: NPC three-level inverters fed dual-three phase PMSM [113]

4.3 Power semiconductor device

In addition to investigating fault-tolerant topologies and control techniques, there are other components to be studied to improve efficiency and performance of a motor, such as EMI filters integrated into the inverter/converter topology to control EMI generated due to device switching. [128]

In the automotive world there is a need for high-power switching devices at higher operating temperatures, this has led to the search for materials for semiconductor devices. Need to mention silicon carbide (SiC) and gallium nitride (GaN), which could replace Silicon (Si).

Silicon and silicon carbide are widely used by power MOSFET devices, thanks to their low-power loss and high-power efficiency [129].

Few researchers have compared the properties of the devices.

A first difference to be highlighted is the high-temperature characteristic, using the same structure and at the same operating condition, the SiC MOSFET temperature is much lower than Si device. Even if with the increase of the temperature, the thermal conductivity decreases but, the thermal conductivity of SiC device is always higher than Si. Another point in favor of SiC power MOSFET is that it will lose less energy in the operating process. [129], [130].

Due to their higher switching frequencies compared to Si IGBTs, SiC MOSFETs prove

to be optimal for applications requiring precise motor control. Additionally, SiC MOSFETs offer a significant advantage over Si IGBT motor driver systems as they can be seamlessly integrated into motor assemblies, housing both the motor controller and inverter within the same unit.

The term "WBG" typically encompasses SiC MOSFETs and GaN HEMTs, which are widely used semiconductor switches in the WBG device market. These wide bandgap modules exhibit superior performance in terms of losses, breakdown voltage, switching frequency, and their ability to withstand higher junction temperatures, as compared to traditional silicon modules. However, employing a WBG device with a high switching frequency at relatively high voltages introduces the challenge of a high derivative of voltage over time, known as dv/dt [127].

Chapter 5
Other multi-phase motors

5.1 Induction motor

The operating principle of an induction motor is based on the induction of a rotating magnetic field in the stator that interacts with the rotor to produce mechanical motion.

The stator is the stationary part of the motor and typically consists of a laminated iron core with evenly spaced windings. These windings are connected to an alternating current (AC) power supply.

When AC power is applied to the stator windings, it creates a rotating magnetic field due to the alternating nature of the current. [117]

The rotor, which is the rotating part of the motor, is typically made of a series of conductive bars or coils placed in slots around an iron core. The rotor is free to spin within the motor. Rotating magnetic field in the stator induces voltage in the rotor conductors through electromagnetic induction. As a result, current starts flowing in the rotor conductors. Current flowing in the rotor conductors interacts with the magnetic field, producing a torque that causes the rotor to turn. The direction of the torque is such that it tries to catch up with the rotating magnetic field in the stator.

The rotor never catches up entirely with the rotating magnetic field so there is always a speed difference between the rotating magnetic field in the stator and the rotor. This speed difference is essential for the motor to generate torque continuously.

The difference between the speed of the rotating magnetic field and the actual rotor speed is known as slip. A small amount of slip is necessary for the motor to operate effectively. The interaction between the rotating magnetic field and the

rotor currents generates a torque in the rotor. This torque is responsible for the mechanical output of the motor.

It worths to highlight the distinction in how the rotor is powered and responds to the stator's magnetic field. The induction motor induces current in the rotor, while the PMSM relies on the magnetic interaction between the stator and the embedded permanent magnets in the rotor.

In recent times, researchers have shown interest in multi-phase induction motors due to their increasing utility in various industrial applications. These motors have gained attention for their notable features, which encompass low torque ripple, superior efficiency when compared to their three-phase counterparts, heightened power density, and enhanced reliability. Specifically, among the multi-phase induction motors, those with a 3k-phase configuration (where k is equal to 2, 3) stand out as an excellent choice for industrial use. This preference comes from their adaptability to standard three-phase induction motor cores, making them well-suited for applications requiring rewinding.[114] To mention the induction motor, the seven-phase motor not yet described above is explored.

5.1.1 Seven phase induction motor

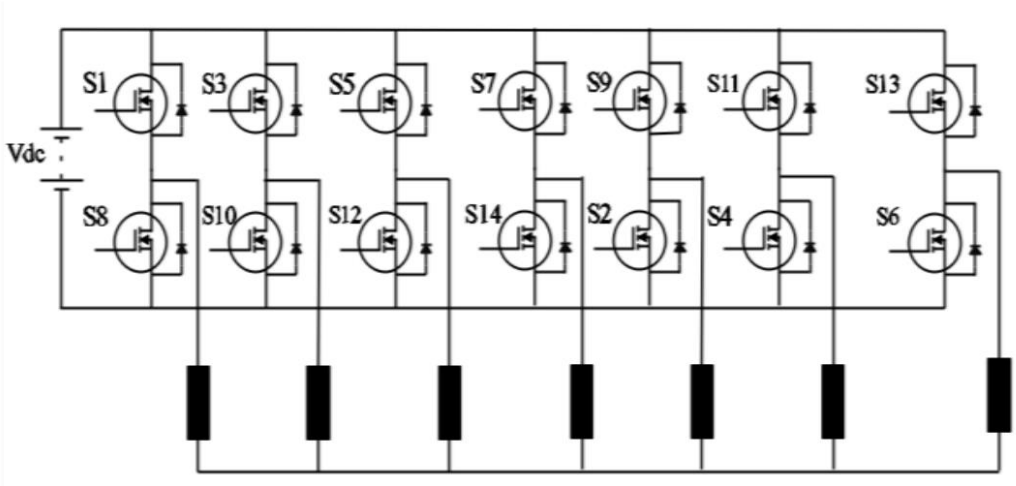

Figure 46: Seven-phase voltage source inverter [115]

Concerning VSI, the power output aligns with that of a traditional 3-phase inverter. When a seven-phase (7ϕ) configuration is required, the power is distributed across the seven arms (depicted in *figure 46*). This distribution enables a reduction in the current load on individual components, potentially leading to lower component ratings. Consequently, there is a likelihood of an overall decrease in the ratings of the switching components.

The equilibrium state of the seven-phase induction motor involves stator coils spaced at intervals of 51.42°. The induction motor's voltage and torque equations incorporate the impact of mutual inductances, which vary over time.[115]

In balanced operating conditions, the stator voltages of the seven-phase induction motor are as follows [115],[116]:

$$V_{as} = V_m \sin(2\pi f t) \tag{5.1}$$

$$V_{bs} = V_m \sin(2\pi f t - {}^{2\pi}/_{7}) \tag{5.2}$$

$$V_{cs} = V_m \sin(2\pi f t - {}^{4\pi}/_{7}) \tag{5.3}$$

$$V_{ds} = V_m \sin(2\pi f t - {}^{6\pi}/_{7}) \tag{5.4}$$

$$V_{es} = V_m \sin(2\pi f t + {}^{2\pi}/_{7}) \tag{5.5}$$

$$V_{fs} = V_m \sin(2\pi f t + {}^{4\pi}/_{7}) \tag{5.6}$$

$$V_{gs} = V_m \sin(2\pi f t + {}^{6\pi}/_{7}) \tag{5.7}$$

The transformation matrix to transform 7ϕ stator variables into two-phase stationary reference frame d-q variables is given 5.8:

$$c = \sqrt{\frac{2}{7}}\begin{bmatrix} 1 & \cos\alpha & \cos 2\alpha & \cos 3\alpha & \cos 3\alpha & \cos 2\alpha & \cos\alpha \\ 0 & \sin\alpha & \sin 2\alpha & \sin 3\alpha & -\sin 3\alpha & -\sin 2\alpha & -\sin\alpha \\ 1 & \cos 2\alpha & \cos 4\alpha & \cos 6\alpha & \cos 6\alpha & \cos 4\alpha & \cos 2\alpha \\ 0 & \sin 2\alpha & \sin 4\alpha & \sin 6\alpha & -\sin 6\alpha & -\sin 4\alpha & -\sin 2\alpha \\ 1 & \cos 3\alpha & \cos 6\alpha & \cos 9\alpha & \cos 9\alpha & \cos 6\alpha & \cos 3\alpha \\ 1 & \sin 3\alpha & \sin 6\alpha & \sin 9\alpha & -\sin 9\alpha & -\sin 6\alpha & -\sin 3\alpha \\ 1/\sqrt{2} & 1/\sqrt{2} & 1/\sqrt{2} & 1/\sqrt{2} & 1/\sqrt{2} & 1/\sqrt{2} & 1/\sqrt{2} \end{bmatrix}$$

(5. 8)

After many calculations the torque can be computed:

$$T_e = pL_m\left[i_{dr}i_{qs} - i_{ds}i_{qr}\right]$$

(5. 9)

It is possible to note that induction motors rely on the induction of current in the rotor to generate torque, PMSMs instead utilize permanent magnets to create a fixed magnetic field in the rotor, leading to differences in control strategies, efficiency, and performance characteristics between the two motor types.

5.2 Reluctance motor

The switched reluctance motor (SRM) is an electrical machine that converts reluctance torque into mechanical power. Its unique design features salient poles in both the stator and rotor, which promote high torque output due to pole alignment. The rotor adjusts to minimize reluctance, maximizing the inductance of the excited winding.[120]

Main advantages of SRM are a simple design of the rotor, the absence of windings and permanent magnets on the rotor, a small moment of inertia of the rotor. Through the absence of windings on the rotor, this type of machine has a high efficiency, and it is characterized by a smaller value of overheating of the

stator winding.[122].

The control of SRM is highly dependent on its design; it follows that design procedures can be complicated.[118]

In SRMs, the stator and rotor poles are typically arranged symmetrically and evenly distributed around the circumference. In traditional three-phase SRMs, commonly used combinations include 6 stator poles and 4 rotor poles or 6 stator poles and 8 rotor poles, denoted as 6/4 or 6/8 stator/rotor configurations.

Similarly, when the phase number exceeds three, it is referred to as a multi-phase SRM (MSRM). The structure of MSRMs resembles that of three-phase SRMs, with the phase number defined as:

$$m = \frac{Z_S}{|Z_S - Z_R|} \tag{5.10}$$

where Z_S and Z_R represent the numbers of stator and rotor poles, and m is the phase number.

Generally, the number of stator poles and rotor poles can be expressed as:

$$Z_S = 2km \tag{5.11}$$

And

$$Z_R = k(2m \pm 2) \tag{5.12}$$

where k is the multiple of the basic combination of stator and rotor poles.

For example, in four-phase SRMs, the combination of stator and rotor poles can be 8/6 or 8/10, and when k=2, the combination becomes 16/12 or 16/20.

SRMs are categorized into two types based on phase numbers: even-numbered phase and odd-numbered phase SRMs.

In odd-numbered phase SRMs, such as three-phase SRMs (*figure 47 a*), the

arrangement of stator magnetic polarity is typically NSNSNS (defined as NS mode), resulting in a symmetrical magnetic field.

In even-numbered phase SRMs, like six-phase SRMs (*figure 47 b*), the stator magnetic polarity arrangement is usually NS mode, leading to an unsymmetrical magnetic field. This can generate mutual inductance between phases, reducing fault tolerance. [119]

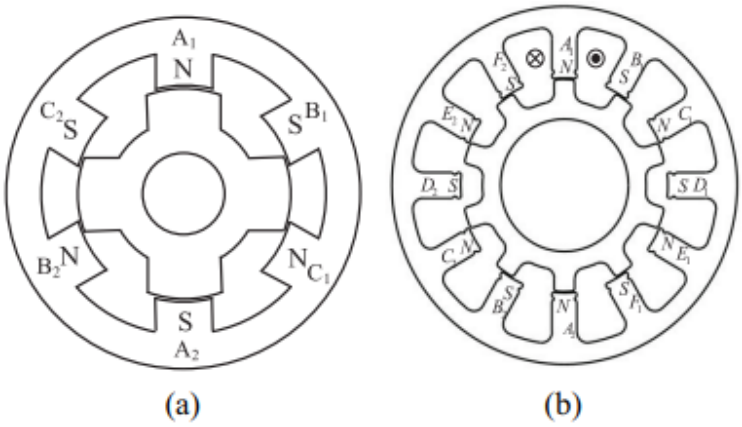

Figure 47: The arrangement of (a) three-phase SRM and (b) six-phase SRM in NS mode [119]

A comparison of four-, five- and six-stage SRM is presented in [118].

To keep all motors at the same rated conditions, the number of turns in the windings must change to obtain the same voltage and current in all phases (the six-phase motor has a lower number of windings turns).

The main differences are summarized which are derived from a finite elements analysis (FEA).

The five-phase SRM is lighter and has a lower moment of inertia. It uses significantly less copper than the other SRMs. However, it has more phases and more poles than the four-phase SRM. In terms of winding resistances, the four-phase SRM has the lowest resistance, and it has the highest efficiency and lowest losses, since it has the lowest current density; nonetheless, the five-phase SRM uses less copper than the four-phase SRM, its current density is much

higher than the four-phase SRM and thus generates more losses. Six phase SRM produces the biggest average output torque.
So, depending on the application, the most appropriate number of phases can be selected to take advantage of its benefits.

5.3 Axial flux motor

Permanent magnet machines are divided into two primary categories based on the direction of the flux passing through the machine's air gap: radial flux machines and axial flux machines. In radial flux machines, the flux travels through the air gap in a radial direction, whereas in axial flux machines, the predominant flux path is axial.
In Axial Flux PM machines, there are two techniques for integrating permanent magnets onto the rotor. The first method involves mounting the magnets on the rotor core, with variations in shape and size depending on the machine's application. In the interior PM type machine, magnets are embedded within the iron core of the rotor, enhancing mechanical strength.
Axial Flux machines can be produced with or without slots. The slotted configuration introduces undesirable elements such as flux ripple, tooth losses, and cogging torque. However, the positive aspect of having a slotted stator is increased robustness and a smaller effective air gap. In the slot-less design, the effects associated with slots are eliminated, resulting in higher overall efficiency. The primary drawback of this machine is its lower mechanical strength. [131]
Axial flux motor control utilizes pulse width modulation inverters, like the control of three-phase radial flux motors. These inverters transform the constant battery voltage into a three-phase power supply with variable frequency and voltage. Torque control is accomplished using the field-oriented technique, enabling precise torque regulation in both steady-state and transient conditions. The flux-weakening operation, activated upon reaching maximum voltage, is executed by manipulating the flux current component.[132]
In the area of axial flux motors, it is worth mentioning YASA (Yokeless and

Segmented Armature) Limited, British manufacturer of electric motors, a founded in September 2009 to commercialize the axial flux permanent magnet electric motor. YASA promises up to four times more power than those commonly used in current electric vehicles. Engines also about 50 percent smaller and lighter.

Chapter 6
Discussion

Combining advantages such as high efficiency, power factor and higher torque density, PM machines offer a full range of benefits. The use of high-energy PM excitation not only reduces overall volume and weight, but also minimizes stator losses, helping to increase efficiency. The absence of rotor copper losses provides an additional increase in efficiency.

PMSMs, with their various characteristics, have applications in various fields. However, their specific advantages make them suitable for traction needs. [1], [86].

It is widely believed that electrification of vehicles will improve performance, energy conservation, and reduce pollutant emissions. Currently, vehicle electrification research and development are largely underway for civilian vehicles, military vehicles, and for specialized areas such as construction vehicles, rail vehicles, and agricultural vehicles.

These efforts focus primarily on the electrification of vehicle traction systems, including electric traction, hybrid electric traction, and fuel cell traction. The main objectives focus on achieving high efficiency and low emissions, maintaining a compact and simple structure, and ensuring good reliability and low cost. [87]

As mentioned above, multiphase machines can be employed, which provide greater freedom in fault management and offer inherent advantages, such as improved reliability, reduced phase current without increased phase voltage, and mitigation of torque ripple. [5]

Typically, two-level 3-phase inverters are preferred due to their mature technology and relatively simple design and control [72].

In a study presented in [67], it was demonstrated that the conduction loss in the two-level configuration is lower than in the NPC three-level configuration. However,

when considering switching power loss and total power losses, the NPC three-level configuration exhibits lower losses than the two-level converters for selected devices. Conversely, the evaluation indicates that the total cost of the switching devices required for the two-level converter is approximately 25% cheaper than that of the three-level converters.

The potential for multi-phase systems to reduce the DC link capacitor has been identified, although the extent of this reduction is case-specific [66].

Other impactful factors are cost and compactness, which play a crucial role in the success of electric drives for hybrid electric vehicles.

To increase system power density, the emphasis is on system integration, which involves incorporating the electric machine, inverter, control, and transmission into a common housing. Inverter integration is facilitated by multiphase motors, which allow a reduction in phase powers and, consequently, inverter modules.[109]

The evolution of hybrid vehicles has been marked by significant milestones and technological advancements.

An interesting excursus is presented in [1]. Toyota initiated its exploration into Hybrid Electric Vehicles (HEVs) before the introduction of the Prius in 1997, the automotive landscape witnessed a paradigm shift. The Prius, launched in 2003, emerged as the world's first full-hybrid vehicle, introducing features like complete electric traction, regenerative braking, and automatic energy preference.

The series-parallel architecture of the Prius, employing two Interior Permanent Magnet (IPM) machines coupled to an Internal Combustion Engine (ICE), set a precedent for future hybrid designs. Notable improvements included the introduction of a boost converter, optimizing power-to-weight ratios, and addressing energy efficiency concerns.

Expanding beyond the Prius, Toyota's SUV models, exemplified by the Toyota Highlander, added complexity due to larger dimensions and increased performance demands. Lexus models, like the RX400h and GS450h, showcased advancements such as improved hybrid systems with PM rotor configurations and enhanced power-to-volume ratios.

Honda's Civic Hybrid brought performance enhancements with high torque at low speed, while the Peugeot Citroen (PSA) group explored diesel ICEs in hybrids, deviating from the convention of gasoline engines.

6.1 Field of application

Nowadays, the drive motors adopted in the automotive sector have traditionally been three-phase PMSMs or induction motors, with the former often preferred for their higher efficiency and power density. Multi-phase drives have traditionally been adopted for high-power wind turbines and marine propulsion, but they are gradually becoming attractive in the automotive sector as well [65].

6-phase motors are said to be the best trade-off between the benefits of multi-three phase machines and the increased system complexity, permitting a relatively easy transition from the traditional 3-phase drives [24].

In [124] the electric vehicle market from 2010 to 2020 is analyzed, and through *figure 48* it can be concluded that, as mentioned above, PMSM has become the first choice of electric vehicle manufacturers due to the high torque and high-power density enabled by high energy density PMs such as neodymium Fe boron and samarium cobalt.

Motor performance is related to energy recovery, which has become a new challenge for EV engines. According to the analysis of [125], the energy recovered from braking is proportional to the torque and efficiency of the motor, and the effect of regenerative braking is best in the constant power region near the base speed. Therefore, to improve the energy recovery effect of regenerative braking, the EV motor must have as wide a constant power range as possible, in addition to maximum efficiency. The IM energy recovery rate is affected by low efficiency, which also reduces the power output and shortens the constant power range. Even if he SRM has a wide speed range its low torque capacity limits the energy recovery effect.

EV model	Power(kW)	Motor	Year
Mahindra e2o Plus	19-30	IM	2016
Renault Kangoo ZE	44	PMSM	2011
Mitsubishi i-MiEV	47	PM	2010
Volkswagen E-up	60	PMSM	2019
Renault Zoe	65	PMSM	2012
LandRover	70	SRM	2013
Renault Fluence Z.E.	70	PMSM	2012
Nissan Leaf	80	PMSM	2010
BJEV EC5	80	PMSM	2019
Hyundai Ioniq Electric	88	PMSM	2016
Hyundai Kona	88-150	PMSM	2018
BYD E6	90	PMSM	2014
BMW i3	125	PMSM	2013
Xpeng G3	139	PMSM	2018
Mercedes-Benz EQC	150*2	IM	2019
BJEV EU5	160	PMSM	2018
Tesla Model X	193-375	IM	2015
Tesla Model 3	211-340	PMSM	2020
Tesla Model S	235-568	IM	2012
NIO EC6	320	PMSM	2020

Figure 48: Example of EVs on the market from 2010 to 2020, includingtheir model, motor categories, and power [124]

Other electric and hybrid vehicles so employ three-phase PMSMs. Notable instances include:

- Audi e-Tron
- Jaguar i-PACE
- Porsche Taycan
- Mercedes EQC

While the Audi e-tron, Jaguar i-Pace, and Mercedes EQC use packs with lithium-ion cells and 400-volt system, specifically 405 volts for EQC, 396 volts Audi e-tron, and 400 volts Jaguar i-Pace, Porsche boasts of being the first manufacturer to implement a voltage level of 800 volts, which turns out to be one of the challenges of the automotive world.

As it is said before, an interesting challenge is the regenerative braking. When the accelerator pedal is released, the electric motor enters generator mode and allows the permanent magnets to induce voltage and current in the stator winding, allowing energy recovery by recharging the lithium-ion battery.

Energy storage plays a crucial role in hybrid electric drivetrains, with chemical batteries commonly utilized in most vehicles. An alternative to consider is the ultracapacitor, known for its high specific power, efficiency, temperature adaptability, and extended lifetime.

Compared to ultracapacitors, the chemical has a much higher specific energy but much less specific power. When chemical batteries need large weight to meet the power requirement, the ultracapacitor needs weight to meet the energy requirement.

Combining ultracapacitors with chemical batteries in a hybrid energy storage system, as in *figure 49*, can achieve a balance, providing both high power and high energy capabilities. This integrated approach also addresses the weight-related challenges [62].

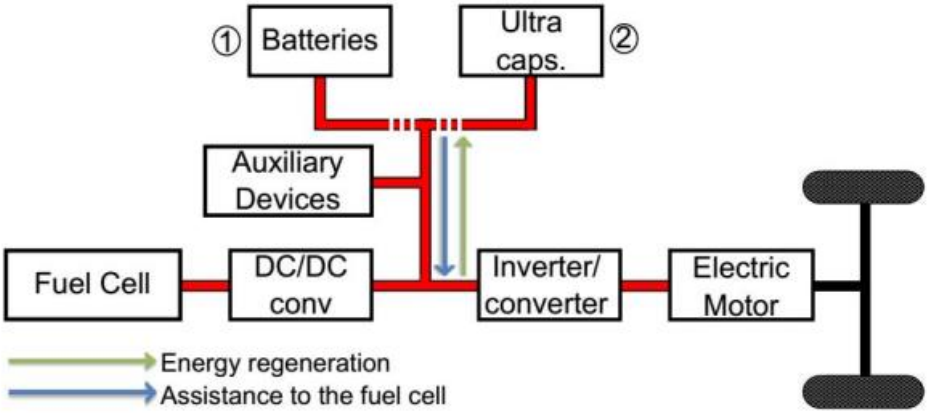

Figure 49: Configuration with combined ultracapacitor and battery [123]

An example of an electric vehicle under development is the e-Axle, depicted in *figure 50*, equipped with a 6-phase buried permanent magnet synchronous motor (BPMSM) powered by a high-efficiency silicon carbide (SiC) inverter and a high-speed transmission and gearbox. The 6-phase inverter is connected to the battery through a DC/DC converter, which raises the battery voltage (400 V) to a maximum of 750 V, to ensure high dynamic performance.

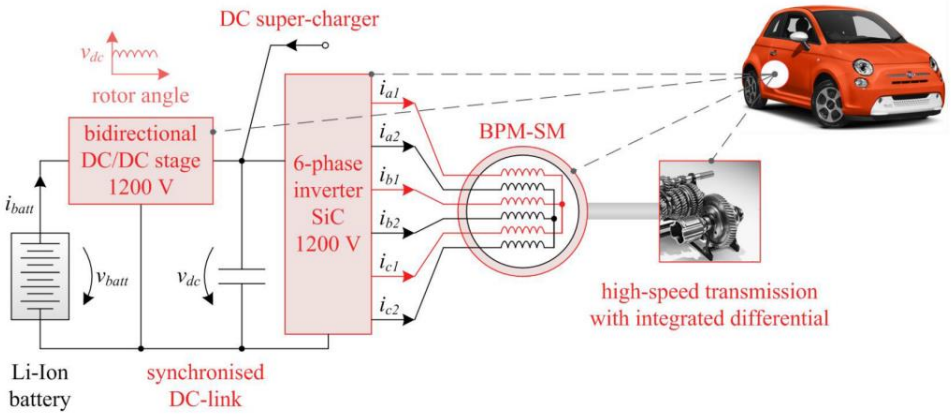

Figure 50:EV on-board architecture [24]

6.2 Summarizing table

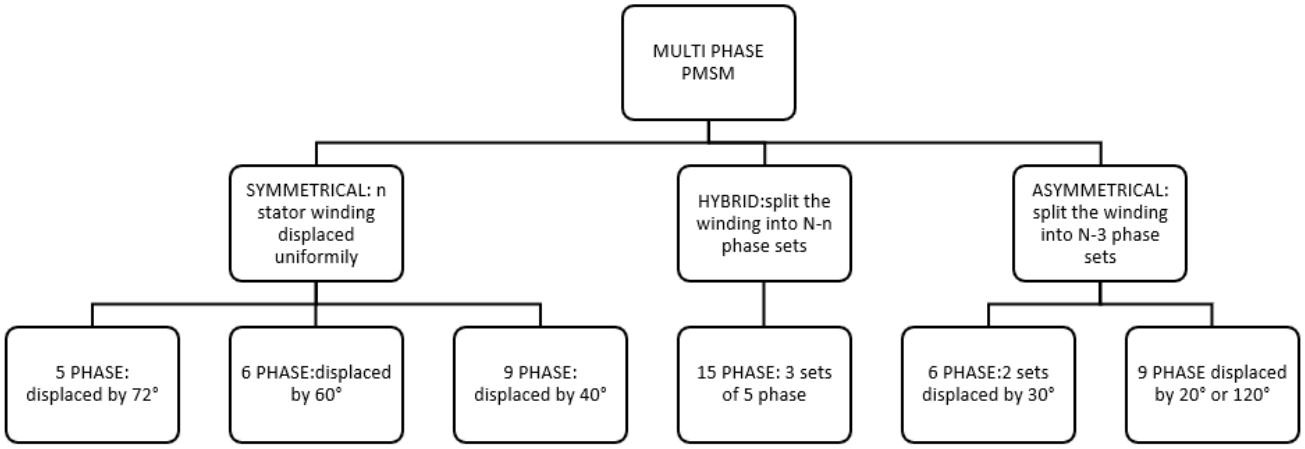

Figure 51:Conceptual map of the topologies covered

Property	Three phase PMSM	Five phase PMSM	Six phase PMSM	Nine phase PMSM
Torque	$T = \frac{3}{2}px$[1]	$T = \frac{5}{2}px$	$T = \frac{6}{2}px$	$T = \frac{9}{2}px$
Power per phase	$P/3$	$P/5$	$P/6$	$P/9$
Phase current	i[2]	$\approx 0.6\ i$	$\approx 0.5\ i$	$\approx 0.35\ i$
DC link capacitance	C[3]	$\approx 0.55\ C$	$\approx 0.5\ C$	$\approx 0.5\ C$
Continued operation after an open phase fault	No	Yes	Yes	Yes

Table 3: Overview of main advantages of multiphase-machine-based drives

[1] $x = (\lambda_p i_q + L_d - L_q) i_d i_q$ having considered dq model with any contribution of the harmonics.
[2] The base value for the current is set for the three-phase case.
[3] The base value for the capacitance is set for the three-phase case.

	Two level inverters	Five-leg inverter	Dual supply inverter	Multilevel inverter
Number of switches	12 for six phase PMSM	10 for six phase PMSM	24 for six phase PMSM	20 for five phase PMSM, 24 for six phase PMSM, 36 for nine phase PMSM
Advantages	Low current for semiconductor, high fault tolerance and simple controller	Less legs and power switches	Suppress some harmonics, isolated DC source	Low voltage stress on power device, robust fault tolerant, individual and flexible control of each phase and reduced thermal stress pull up the voltage and the power level
Disadvantages	High complexity due to the number of legs that depend on number of phases	Find a balanced midpoint voltage	Additional capacitor bank	Multitude of voltage vector that must be reduced

Table 4: Overview of inverter topologies

Characteristics	PMSM	Induction motor	Switched reluctance motor
Operating principle	The stator windings generate a rotating magnetic field whose polar expansions interact with the PM in the rotor	Rotating magnetic field in the stator induces voltage in the rotor conductors through electromagnetic induction	Converts reluctance torque into mechanical power
Rotor topology	PM buried inside the rotor or surface mounted	Conductive bars or coils	Salient pole
Efficiency	High efficiency due to the excitation of the PM	Influenced by slip and by electrical losses due to the	Depends on the optimization of pole alignment

		induced current	
Torque ripple	Low	Moderate and may require additional measurement	Minimized by the rotor adjustment
Advantages	High torque, efficiency and power factor	Self-startup, simpler	Simple design of the rotor, high efficiency, and smaller value of overheating of the stator winding.
Disadvantages	Cost of PM and complexity in control	Rotor losses associated to induced current	Complicated design procedure

Table 5: Comparison between different type of machine

6.3 Conclusion

In [64] an excursus over time of various steps that led to the validation of the improvements made by multiphase motors is presented.

In the 1960s, Ward and Harer conducted theoretical and experimental analysis on five-phase induction machines, discovering that an increase in phase number reduces torque ripple amplitude but increases frequency. The concept of multiphase drives emerged in 1980 to enhance fault tolerance and reliability, facing implementation challenges at the time. Technological advancements since the 1990s, including power electronics and microcontrollers, facilitated the development of multiphase drives.

Over the last thirty years, extensive research globally has resulted in novel designs, converter topologies, and control methods for multiphase machines. Notable contributions include fault-tolerant control strategies, Pulse Width Modulation techniques, and Model Predictive Control strategies. Chinese researchers, including those from the Naval University of Engineering and Harbin Institute of Technology, have actively explored mathematical models, fault characteristics, and various machine topologies for multiphase drives.

With increasing user demands for reliability and safety in installed drives,

manufacturers of control systems for AC drives are increasingly focusing on incorporating diagnostic functions into their converter control algorithms.

The ongoing advancements in sensor technology, measuring equipment, digital signal processing software, and computational intelligence allow continuous monitoring of drive conditions and trend observation [110].

The classic and dynamic control techniques for PMSM are vector control i.e., field-oriented control and direct torque control that require the rotor position to generate the reference current which in effect produces the required torque. [23]

The future challenges therefore include system complexity, control techniques, cost increase, sensor technologies and diagnostic function.

It is important to remember the selection of power semiconductor devices, control and switching strategies, the packaging of the individual units, and the system integration especially when it comes to efficient and high-performance vehicles.[128]

The inherent advantages of permanent magnet machines, high torque and efficiency, combined with those of multiphase machines, improved reliability, phase current reduction, torque ripple attenuation, extra degree of freedom, make multi-phase PMSMs worthy of further study to become the future of electric machines and beyond.

Bibliography

[1] Massimo Barcaro and Nicola Bianchi «PM Motors for Hybrid Electric Vehicles », Published in: 2008 43rd International Universities Power Engineering Conference.

[2] Z. Q. Zhu, Senior Member IEEE, and David Howe «Electrical Machines and Drives for Electric, Hybrid, and Fuel Cell Vehicles», Published in: Proceedings of the IEEE, Vol. 95, Issue: 4, pp. 746 – 765.

[3] Dr. Karunamoorthy, B. and *Dhivyaa, D. « PMSM and its application», Published in: May, 2017, International Journal of Current Research Vol. 9, Issue:05, pp.51047-51050.

[4] Gurakuq Dajaku and Dieter Gerling «Low Costs and High-Efficiency Electric Machines», Published in: 2012 2nd International Electric Drives Production Conference (EDPC)

[5] Guang Jin Li, Bo Ren, Zi Qiang Zhu. «Design guidelines for fractional slot multi-phase modular permanent magnet machines »,Published in: July 2017, Volume11, Issue6, ,pp. 1023-1031.

[6] Tahir Aja Zarma, Ahmadu Adamu Galadima1and Maruf A. Aminu «Review of Motors for Electric Vehicles», Published in: *Journal of Scientific Research and Reports*, Volume 24, Issue 6, pp. 1-6.

[7] X.T. Garcia, B. Zigmund, A. Terlizzi, R. Pavlanin, L. Salvatore «Comparison between FOC and DTC strategies for permanent magnet synchronous motors», pp. 76-81.

[8]Amelia Carolina Sparavigna «Ferraris-Zähler, il contatore di Galileo Ferraris: Stralci dalla letteratura sulla scoperta del campo magnetico rotante », 2019.

[9] M. Mitolo and M. Tartaglia «Galileo Farraris - A Life Dedicated to the Electric Sciences [History] », Published in: Sept.-Oct. 2016, IEEE Industry Applications Magazine Volume: 22, Issue: 5, pp. 8 – 11.

[10] R. Krishnan «Permanent Magnet Synchronous and Brushless DC Motor Drives», Published in: 2010 by Taylor and Francis Group, LLC. pp.52.

[11] M. Barcaro, N. Bianchi, F. Magnussen «Six – phase supply feasibility using a PM fractional – slot dual winding machine»,Published in :Sept.-Oct. 2011,IEEE Transactions on Industry Applications, Vol. 47, Issue: 5,), pp. 2042–2050.

[12] Jianning Dong; Yunkai Huang; Long Jin; Heyun Lin «Comparative Study of Surface-Mounted and Interior Permanent-Magnet Motors for High-Speed Applications», Published in: June 2016,IEEE Transactions on Applied Superconductivity (Volume: 26, Issue: 4).

[13] Jingliang Lv;Gangling Tian;Xinjian Jiang;Wencan Li;Xinzhen Zhang;Zhehui Niu;Jianyun Chai «Fault-Tolerant Control of Twelve-Phase PMSM Based on Motor Model Reconstruction in FESS», Published in: 2020 IEEE 4th Conference on Energy Internet and Energy System Integration (EI2) pp.3703-3708.

[14] Sukanta Halder; S.P. Srivastava; Pramod Agarwal « Flux Weakening Control Algorithm with MTPA Control of PMSM Drive » Published in: 2014 IEEE 6th India International Conference on Power Electronics (IICPE).

[15] M. Onsal; Y. Demir; M. Aydin «A New Nine-Phase Permanent Magnet Synchronous Motor With Consequent Pole Rotor for High-Power Traction Applications», Published in: November 2017, IEEE Transactions on Magnetics,Vol.: 53, Issue: 11.

[16] Dongyun Lu; Narayan C. Kar «A Review of Flux-weakening Control in Permanent Magnet Synchronous Machines» Published in: 2010, IEEE Vehicle Power and Propulsion Conference.

[17] M. Caruso, A. O. Di Tommaso, R. Miceli, C. Nevoloso, C. Spataro, M. Trapanese, Maximum Torque per Ampere Control Strategy for Low-Saliency Ratio IPMSMs », Published in:2019 INTERNATIONAL JOURNAL of RENEWABLE ENERGY RESEARCH., Vol.9, No.1 pp.374-383.

[18]A. Tessarolo «Benefits of increasing the number of stator phases in terms of winding construction technology in high-power electric machines, Published in: 19-21 April 2010, 5th IET International Conference on Power Electronics, Machines and Drives (PEMD 2010).

[19]L. Parsa «On Advantages of Multi-Phase Machines» Published in: November 2005,31st Annual Conference of IEEE Industrial Electronics Society. IECON 06-10.

[20] Yuriy Kats «Adjustable-Speed Drives With Multiphase Motors», Published in: 1997 IEEE International Electric Machines and Drives Conference Record

[21] Saeid Haghbin; Torbjorn Thiringer; Ola Carlson «An integrated split-phase dual-inverter permanent magnet motor drive and battery charger for grid-connected electric or hybrid vehicles », Published in: 2012 XXth International Conference on Electrical Machines.

[22] Carlos Miguel-Espinar; Daniel Heredero-Peris; Gabriel Gross; Marc Llonch-Masachs;« Maximum Torque per Voltage Flux-Weakening Strategy With Speed Limiter for PMSM Drives », Published in:2021, IEEE Transactions on Industrial Electronics ,Vol. 68, Issue: 10,pp.9254 - 9264.

[23] Rishi Menon; Arvind H. Kadam; Najath Abdul Azeez; Sheldon S. Williamson , « A Comprehensive Survey on Permanent Magnet Synchronous Motor Drive Systems for Electric Transportation Applications », Published in: IECON 2016 - 42nd Annual Conference of the IEEE Industrial Electronics Society, pp.6627-6623.

[24] M. Martino, P. Pescetto, and G. Pellegrino, «Advanced functionally integrated e-axle for A-segment electric vehicles », Published in: 2020, Proc. AEIT Int. Conf. Electr. Electron. Technol. Automot. (AEIT AUTOMOTIVE), pp. 1–6

[25] Stefan Piepenbreier;Julian Berlinecke;Nicola Burani;Roland Bittner; Serhij Matichyn; Fabian Streit; Maximilian Hofmann; Robert Plikat «Analysis of a multiphase multi-star PMSM drive system with SiC-based inverter for an automotive application» Published in: PCIM Europe 2018; International Exhibition and Conference for Power Electronics, Intelligent Motion, Renewable Energy and Energy Management.

[26] L. Parsa and H. Toliyat, «Multi-phase permanent magnet motor drives» Published in: 2003, Industry Applications Conference, 38th IAS Annual Meeting. Conference Record of the Industry Applications Conference, vol. 1, pp. 401 – 408.

[27]E. Levi, «Multiphase electric machines for variable-speed applications» Published in: may 2008Industrial Electronics, IEEE Transactions on Industrial Electronics, vol. 55, no. 5, pp. 1893 –1909.

[28] T. G. Wilson; P. H. Trickey, «DC motors with solid-state commutation», Published in: November 1962, Electrical Engineering,Vol. 81, Issue: 11, pp.879 – 884.

[29] Zhao, J., Liu, Y., Xu, X. «Comparisons of Concentrated and Distributed Winding PMSM in MV Power Generation», Published in: 2018, XIII International Conference on Electrical Machines (ICEM), pp. 2437-2443.

[30] Alberto Tessarolo, Cesare Ciriani, Mauro Bortolozzi, Mario Mezzarobba, Nicola Barbin, «Investigation Into Multi-Layer Fractional-Slot Concentrated Windings With Unconventional Slot-Pole Combinations», Published in: December 2019,IEEE Transactions on Energy Conversion,Vol. 34, Issue: 4, pp. 1985 – 1996.

[31] Ei Kyaw Aung Nay Tun, Thet Tin, «Design of Conventional Permanent Magnet Synchronous Motor used in Electric Vehicle», Published in: July-2014, International Journal of Power Electronics and Drive Systems, ISSN 2319-8885 , Vol.03,Issue.16 pp. 3289-3293.

[32] Daniel Keller; Akif Karayel; Nejila Parspour; «Application of an accurate calculation method for dual three-phase PMSM», Published in: 2021, IEEE Workshop on Electrical Machines Design, Control and Diagnosis (WEMDCD), pp.34-392.

[33] Daniel Keller; Moritz Kuenzler; Akif Karayel; Quentin Werner; Nejila Parspour; «Potential of Dual Three-Phase PMSM in High Performance Automotive Powertrains», Published in: 2020 International Conference on Electrical Machines (ICEM), pp. 1800-1806.

[34] Dinh, Bui Minh and Quyet, Dinh Xuan, «Line Start Permanent Magnet Synchronous Motor for Underground Mining Drive Application», Published in: 2021, Proceedings of the International Conference on Industrial Engineering and Operations Management Rome, Italy, pp. 1676-1684.

[35] Merrill, «Permanent-Magnet Excited Synchronous Motors», Published in: Feb. 1955, Electrical Engineering, Voi. 74.

[36] Badreddine NAAS, L. NEZLI, Bachir NAAS, M.O. MAHMOUDI, M. ELBAR, «Direct Torque Control Based Three Level Inverter-fed Double Star Permanent Magnet Synchronous Machine», Published in: December 2012, Article in Energy Procedia · pp. 521-530.

[37] R. H. PARK, «Two Reaction Theory of Synchronous Machines », July 1929, Published in: Transactions of the American Institute of Electrical Engineers,Vol. 48, Issue: 3, pp-716-727.

[38] T.J.E. Miller and M.I. McGilp, «Analysis of multi-phase permanent-magnet synchronous machines»,Published in: 2009 International Conference on Electrical Machines and Systems.

[39] Bui Minh Dinh; Ho Manh Tien, «Maximum efficiency design of line start permanent magnet synchronous motor», Published in: 2016 IEEE International Conference on Sustainable Energy Technologies (ICSET).

[40] B. K. Bose, «A high-performance inverter-fed drive system of an interior pm synchronous machine, » Published in: Nov/Dec 1988, IEEE Transaction on Industry Application, vol. 24, pp. 987–997.

[41] L. Qinghua, M. A. Jabbar, and A. M. Khambadkone, «Design optimisation of wide-speed permanent magnet synchronous motors», Published in April 2002, Proceedings of International Conference on Power Electronics, Machines and Drives, (Bath, UK), pp. 404–408.

[42] L. Qinghua, M. A. Jabbar, and A. M. Khambadkone, «Design optimisation of interior permanent magnet synchronous motors for wide-speed operation, », Published in: October 2001, Proceedings of the 4th IEEE International Conference on Power Electronics and Drive Systems, (Bali, Indonesia), pp. 475–478.

[43] J. E. Miller, « Brushless permanent-magnet and reluctance motor drive. », Published in: 1989, Oxford, London: Claredon Press.

[44] T. M. Jahns, «Flux-weakening regime operation of an interior permanent magnet synchronous motor drive », Published in:July/August 1987,IEEE Transaction on Industry Application, vol. IA-23, pp. 681–689 .

[45] Osman Emre ÖZÇİFLİKÇİ , Mikail KOÇ, «Analysis of the Saliency Ratio Effect on the Output Torque and the System Efficiency in IPM Drives» Published in: 2021, Sakarya University Journal of Science SAUJS, vol 25, Issue: 6,pp. 1417-14246.

[46] S. Morimoto, M. Sanada, and Y. Takeda, «Wide-speed operation of interior permanent magnet synchronous motors with high-performance current regulator», Published in: July/Aug 1994, IEEE Trans. Ind. Applicat., vol. 30, pp. 920–926.

[47] Ju-Hee Cho; Hong-Seok Oh; Sang-Uk Cho; Deok-Geun-Kim; Ik-Seong Park, «Development of IPM synchronous motor for diesel hybrid electric vehicle»,

Published in: INTELEC 2009 - 31st International Telecommunications Energy Conference.

[48] Ahmed Salem, Mehdi Narimani, «A Review on Multiphase Drives for Automotive Traction Applications», Published in: December 2019, IEEE Transactions on Transportation Electrification, Vol. 5, No. 4, pp. 1329-1348.

[49] H. E. Jordan, R. C. Zowarka, S. B. Pratap, «Nine-phase armature windings design, test and harmonic analysis», Published in: Jan. 2005, IEEE Trans. on Magnetics, vol. 41, issue 1, part 2, pp. 299-302.

[50] F. Terrein, S. Siala, P. Noy, «Multiphase induction motor sensorless control for electric ship propulsion», Published in: IEE Power Electronics, Machines and Drives Conference, PEMD 2004, pp. 556-561.

[51] F. Terrein, S. Siala, P. Noy, «Multiphase induction motor sensorless control for electric ship propulsion», Published in: IEE Power Electronics, Machines and Drives Conference, PEMD 2004, pp. 556-561.

[52] Ranran Wang; Caixia Tao; Fengyang Gao; Weibin Wang; Jiangang Zhang, «Fault-tolerant Control Strategy of Five-phase Permanent Magnet Synchronous Motor ». Published in: 2021 8th International Forum on Electrical Engineering and Automation (IFEEA), pp 577-582.

[53] Yongqing Wei, Mingzhong Qiao, and Peng Zhu, «Fault-Tolerant Operation of Five-Phase Permanent Magnet Synchronous Motor with Independent Phase Driving Control» Published in: 2022, Ces Tralaw:ions On Electrical Machines And Systems, Vol. 6, No. 1 , pp. 105-110.

[54] Sangeeta Sahu; Byamakesh Nayak; Rudra Narayan Dash, «Modeling and Vector Control of Five Phase Surface Permanent Magnet Synchronous Motor». Published in: 2021 Innovations in Energy Management and Renewable Resources (52042).

[55] Ping Zheng; Yi Sui; Jing Zhao; Chengde Tong; T. A. Lipo; Aimeng Wang, «Investigation of a Novel Five-Phase Modular Permanent-Magnet In-Wheel Motor», Published in: October 2011, IEEE Transactions On Magnetics, vol. 47, no. 10,pp. 4084-4087.

[56] Leila Parsa, Hamid A. Toliyat, «Five-Phase Permanent-Magnet Motor Drives», Published in: 2005, IEEE Transactions on Industry Applications, Vol. 41, No. 1, pp. 30-37.

[57] Raja Ram Kumar, Priyanka Devi, Chandan Chetri, Kundan Kumar, «Electromagnetic Characteristics Investigation of Novel Dual Stator Delta-Shaped Magnet Five-Phase Permanent Magnet Synchronous Motor for Electrical Vehicle Application», Published in: 2021 1st International Conference on Power Electronics and Energy (ICPEE-2021).

[58] Yifei Qin; Aiyuan Wang, «Direct Torque Control of Five-phase Permanent Magnet Synchronous Motor Based on Model Prediction», Published in: 2021 International Conference on Machine Learning and Intelligent Systems Engineering (MLISE),pp. 126-130.

[59]Muyang Li,Jiangbiao He,Nabeel Demerdash, «A Flux-Weakening Control Approach for Interior Permanent Magnet Synchronous Motors Based on Z-Source Inverters», Published in: 2014 IEEE Transportation Electrification Conference and Expo.

[60] L. Parsa;N. Kim;H.A. Toliyat, «Field Weakening Operation of a High Torque Density Five Phase Permanent Magnet Motor Drive», Published in: 2005, IEEE International Conference on Electric Machines and Drives, pp. 1507-1512.

[61] L. Parsa;N. Kim;H.A. Toliyat, « Open-circuit fault tolerant control of five-phase permanent magnet motors with third-harmonic back-EMF», Published in: 2008 34th Annual Conference of IEEE Industrial Electronics, pp- 3114-3119.

[62] Mehrdad Ehsani; Yimin Gao; John M. Miller« Hybrid Electric Vehicles:Architecture and Motor Drives», Published in: 2007, Proceedings of the IEEE Vol. 95, Issue: 4,pp.719-728.

[63] Chiao-Chien Lin; Ying-Yu Tzou , «An innovative multiphase PWM control strategy for a PMSM with segmented stator windings», Published in: 2015 IEEE Applied Power Electronics Conference and Exposition (APEC), pp. 270-275.

[64] Zicheng Liu; Yongdong Li; Zedong Zheng , «A review of drive techniques for multiphase machines», Published in: June 2018, CES Transactions on Electrical Machines and Systems Vol. 2, Issue: 2,pp. 243 - 251.

[65] Paolo Pescetto;Matias Fernando Troncoso Cruz;Fausto Stella;Gianmario Pellegrino, «Galvanically Isolated On-Board Charger Fully Integrated With 6

Phase Traction Motor Drives»,Published in: 2023, IEEE Access, Vol. 11, pp. 26059 – 26069.

[66] B. Basler, T. Greiner and P. Heidrich, «Reduction of DC link capacitor stress for double three-phase drive unit through shifted control and phase displacement», Published in: 2015 IEEE 11th International Conference on Power Electronics and Drive Systems, Sydney, NSW, 2015, pp. 887-889

[67] P. Alemi and D. Lee, «Power loss comparison in two- and three-level PWM converters», Published in: 2011, 8th International Conference on Power Electronics - ECCE Asia, pp. 1452-1457.

[68] Raja Ram Kumar; Chandan Chetri; Priyanka Devi; Ankita Dwivedi, «Design and Analysis of Dual Stator Dual Rotor Six-Phase I-Shaped Permanent Magnet Synchronous Motor for Electric Vehicles Application»,Published in: 2020 IEEE International Conference on Power Electronics, Drives and Energy Systems (PEDES).

[69] Dong Ting, Li Fenghui1 and Shen li, « Fault-Tolerant Method for Six-Phase PMSM by Adjusting Phase Angle»,Published in: 2017,20th International Conference on Electrical Machines and Systems (ICEMS).

[70] Yong Chen; Jin-long Song; Jian-jian Zhang; Qiu-liang Huang, «Design and Analysis of Six-phase Fault-tolerant PMSM for Electric Vehicle»,Published in: 2016 Prognostics and System Health Management Conference (PHM-Chengdu).

[71] Elena Macrelli; Alberto Bellini; Claudio Bianchini; Ambra Torreggiani, «Fault Tolerance Analysis of Multiphase Ironless PMSM for Flywheel Batteries»,Published in: 2023 IEEE 14th International Symposium on Diagnostics for Electrical Machines, Power Electronics and Drives (SDEMPED).

[72] Artem Rodionov; Alessandro Acquaviva; Yujing Liu; «Sizing and energy efficiency analysis of a multi-phase FSCW PMSM drive for traction application »,Published in: IECON 2020 The 46th Annual Conference of the IEEE Industrial Electronics Society, pp.2069-2074.

[73] Andrea Del Pizzo; Luigi Pio Di Noia; Antonino Oscar Di Tommaso; Rosario Miceli; Renato Rizzo, «Comparison between 3-ph and 6-ph PMSM drives for the electric propulsion of unmanned aerial vehicles»,Published in: 2021, IEEE 15th International Conference on Compatibility, Power Electronics and Power Engineering (CPE-POWERENG).

[74] Xueqing Wang, Zheng Wang, Pengcheng Liu, Ming Cheng, «A Hybrid Direct Torque Control Scheme for Asymmetric Six-Phase PMSM Drives »,Published in:

IECON 2017 - 43rd Annual Conference of the IEEE Industrial Electronics Society.

[75] Yashan Hu, Z. Q. Zhu, Milijana Odavic, « Comparison of Two-Individual Current Control and Vector Space Decomposition Control for Dual Three-Phase PMSM», Published in: 2017 IEEE Transactions on Industry Applications , Vol. 53, Issue: 5, pp. 4483 – 4492.

[76] Matus Kozovsky, Petr Blaha, Pavel Vaclavek; Lingshun Liu, «Verification of Nine-phase PMSM Model in d-q Coordinates with Mutual Couplings»,Published in: 2016 6th IEEE International Conference on Control System, Computing and Engineering (ICCSCE), pp.73-78.

[77] Shilei Duan , Xinzhen Wu, Haifeng Wang, and Hongheng Wu, « Analysis and Optimization of Open-loop Control Stability of Nine-phase Permanent Magnet Synchronous Motor»,Published in: 2020, 23rd International Conference on Electrical Machines and Systems (ICEMS), pp.1240-1245.

[78] Matus Kozovsky, Petr Blaha and Pavel Vaclav, « Vector Control of Nine-phase Permanent Magnet Synchronous Motor under Symmetrical Fault Condition for Derating Operation»,Published in: 2020 23rd International Conference on Electrical Machines and Systems (ICEMS), pp.2154-2157.

[79] Vasile, E. Tudor, M. Popescu, C. Dumitru, L. Popovici And I. C. Sburlan, « Electric Drives with Multiphase Motors as a Better Solution for Traction Systems, » Published in: 2019 11th International Symposium on Advanced Topics in Electrical Engineering (ATEE), Bucharest, Romania, pp. 1-5.

[80] D. Zhou, Z. Zhao, S. Wang and J. Chai, « Vector control for a twelve-phase synchronous motor, » Published in: 2007 International Conference on Electrical Machines and Systems (ICEMS), Seoul, pp. 1037-1040.

[81] Xudong Zhang; Xiaoqin Zheng; Xiudong Li; Haifeng Wang,« Open-Circuited Faults Diagnosis of a Nine-Phase Permanent Magnet Synchronous Motor Drive System Based on Mean Phase Current »,Published in: 2021, 24th International Conference on Electrical Machines and Systems (ICEMS), pp.961-964.

[82] V. F. M. B. Melo, C. B. Jacobina, and N. B. de Freitas, «Open-end nine phase machine conversion systems, » Published in: 2017, IEEE Trans. Ind. Appl., vol. 53, no. 3, pp. 2329–2341.

[83] Z. Nie, « Multiphase power electronic converters for electric vehicle machine drive systems," » Published in: 2018, Ph.D. dissertation, Dept. Elect. Comput. Eng., McMaster Univ., Hamilton, ON, Canada.

[84] I. Zoric, M. Jones, and E. Levi, «Vector space decomposition algorithm for asymmetrical multiphase machines, » Published in: 2017, Proc. Int. Symp. Power Electron. (Ee), pp. 1–6.

[85] Z. Wang, Y. Wang, J. Chen, and Y. Hu, «Decoupled vector space decomposition-based space vector modulation for dual three-phase three-level motor drives, » Published in: 2018, IEEE Trans. Power Electron., vol. 33, no. 12, pp. 10683–10697.

[86] Enrico Carraro; Michele Degano; Mattia Morandin; Nicola Bianchi, « PM synchronous machine comparison for light electric vehicles, » Published in: 2014 IEEE International Electric Vehicle Conference (IEVC).

[87] M. Ehsani, Y. Gao, and S. Gay, « Characterization of electric motor drives for traction applications,» Published in: 2003,Industrial Electronics Society, IECON '03. The 29th Annual Conference of the IEEE, vol. 1, pp. 891–896.

[88] R. Bojoi, S. Rubino, A. Tenconi, and S. Vaschetto, «Multiphase electrical machines and drives: A viable solution for energy generation and transportation electrification, » Published in: Proceedings of the 2016 International Conference and Exposition on Electrical and Power Engineering, EPE 2016, 2016, pp. 632–639.

[89] Voltage, Current and Power in 3 Phase Star Connection: https://www.eeeguide.com/3-phase-star-connection/

[90] E. E. Ward and H. Härer, «Preliminary investigation of an invertor-fed 5-phase induction motor, » Published in: 1969 Proc. Inst. Electr. Eng., vol. 116, no. 6, pp. 980–984.

[91] J. Wettlaufer, H. Borcherding, F. Klute, and T. Jonsky, «A compact servo drive: five phase, air cooled, with highly integrated inverter for industrial use, » Published in: 17th European Conference on Power Electronics and Applications (EPE'15 ECCE-Europe), Geneva, Switzerland, 2015

[92] Wettlaufer J.; Jonsky T.; Maghnaoui A.: Hernandez R.; Klute F., «Structure of a multi-phase industrial servo drive with highly integrated inverter», Published in: 2015, PCIM Europe 2015, Nuremberg, Germany, pp. 741-748

[93] Jakob Jung, Bernd Cebulski ,« Analytic Design of Multi-Phase Electric Machines with Independent H-Bridge Supply », Published in: 2015, 2018 XIII International Conference on Electrical Machines (ICEM), pp. 2037-2043

[94] Brockerhoff P.; Burkhardt Y.; Egger K.; Rauh H.: « Smart Stator Tooth Design with novel Control and Safety Functions in Electric Vehicle Drivetrains», Published in: PCIM Europe 2015, 19-21 May 2015, Nuremberg, Germany, pp. 691-698

[95] Mohammadpour A,Parsa L., « Global fault-tolerant control technique for multi-phase permanent-magnet machines», Published in: 2015 IEEE Trans. on Industry Applications, vol. 51, no. 1, pp. 178-186.

[96] Klaus Schuhmacher,Emanuele Grasso, Matthias Nienhaus, «Improved rotor position determination for a sensorless star-connected PMSM drive using Direct Flux Control, » Published in: 2019 The Journal of engineering.

[97] Wikipedia, (24 Sept. 2007). AC star connection: File:AC star connection.svg - Wikipedia

[98] A. Rosen, M. Gröninger, A. Mertens, «Modeling and Optimized Control of Fault-Tolerant H-Bridge Fed Multiphase Drives, » Published in:2015, 17th European Conference on Power Electronics and Applications (EPE'15 ECCE Europe), Geneva, Switzerland.

[99] A. Kock, M. Groninger, A. Mertens, «Modeling and Control of Fault Tolerant Drive Topologies for Electric Vehicle Application,» Published in: 2014 International Conference on Electrical Machines (ICEM).

[100] Abdalla Hussein Mohamed; Hendrik Vansompel; Peter Sergeant, «A Generic DC link Capacitor Sizing Methodology for Multi-phase Wide Bandgap Based Integrated Modular Motor Drives, » Published in: 2020 IEEE International Conference on Environment and Electrical Engineering and 2020 IEEE Industrial and Commercial Power Systems Europe (EEEIC / I&CPS Europe).

[101] G. J. Su and L. Tang, «A segmented traction drive system with a small dc bus capacitor, » Published in: 2012 IEEE Energy Conversion Congress and Exposition, ECCE 2012, pp. 2847–2853.

[102]X. Pei, W. Zhou, and Y. Kang, «Analysis and Calculation of DC-Link Current and Voltage Ripples for Three-Phase Inverter With Unbalanced Load, » Published in: 2015, IEEE Transactions on Power Electronics, vol. 30, no. 10, pp. 5401–5412.

[103] Bharath Lingamchetty, Anchal Raghuwanshi, Amit Ojha, «Battery Connected Multi-level Inverter Fed PMSM for Electric Vehicle Applications, » Published in:2023 IEEE Renewable Energy and Sustainable E-Mobility Conference (RESEM).

[104] C. C. Chan, A. Bouscayrol, and K. Chen, «Electric, hybrid, and fuel-cell vehicles: Architectures and modeling, » Published in: 2010, IEEE Transactions on Vehicular Technology, Vol. 59, No. 2, pp. 589–598.

[105] R. Bojoi, S. Rubino, A. Tenconi, and S. Vaschetto, «Multiphase electrical machines and drives: A viable solution for energy generation and transportation electrification, » Published in: Proceedings of the 2016 International Conference and Exposition on Electrical and Power Engineering, EPE 2016,pp. 632–639.

[106] Zhuoyi Chen, Jianqi Qiu and Mengjia Jin, «A PWM Coordination Strategy to Reduce DC-link Capacitor Dependence in Converter-Inverter Systems,» Published in: 2016 IEEE Vehicle Power and Propulsion Conference (VPPC).

[107] H. Ye, A. Emadi, «An interleaving scheme to reduce DC-link current harmonics of dual traction inverters in hybrid electric vehicles, » Published in: 2014, IEEE Applied Power Electronics Conference and Exposition, pp. 3305-3211.

[108] Ali Nurettin Demir, Ahmet Safa Karakoç, Mustafa Turhan, «Design and analysis of an 8 pole 1Kw synchronous PM machine, » Published in: 2022.

[109] Y. Burkhardt, A. Spagnolo, P. Lucas, M. Zavesky, and P. Brockerhoff, «Design and analysis of a highly integrated 9-phase drivetrain for EV applications, » Published in: 2014, IEEE-ICEM, pp. 450–456.

[110] Teresa Orlowska-Kowalska,Marcin Wolkiewicz , Przemyslaw Pietrzak , Maciej Skowron , Pawel Ewert , Grzegorz Tarchala , Mateusz Krzysztofiak , And Czeslaw T. Kowalski, «Fault Diagnosis and Fault-Tolerant Control of PMSM Drives–State of the Art and Future Challenges» Published in: 2022, IEEE Access ,Vol.10, pp. 59979 - 60024.

[111] S. M. Kim and T. Kwon, «A Method to Minimize Current Ripple of DC Link Capacitor for 48V Inverter Integrated Starter/Generator» Published in: 2018 IEEE Energy Conversion Congress and Exposition, ECCE , pp. 3917–3922.

[112] Y. Zhao and T. A. Lipo , «Space vector PWM control of dual three-phase induction machine using vector space decomposition,» Published in: 1995, IEEE Trans. Ind. Appl., vol. 31, no. 5, pp. 1100–1109.

[113] Z. Wang, J. Chen, M. Cheng, and R. Na, «Vector space decomposition-based control of neutral-point-clamping (NPC) three-level inverters fed dual three-phase PMSM drives, » Published in: 2016, in Proc. 42nd Annu. Conf. IEEE Ind. Electron. Soc. (IECON), pp. 2988–2993.

[114] Hadi Aghaei; Ebrahim Babaei; Mohammad Bagher Bannae Sharifian; Ibrahim Shoghli, «Partly Isolated Symmetrical Six-Phase Induction Motor Drive System Based on Conventional Three Phase Transformer», Published in: 2023, The 14th Annual Power Electronics and Drive: Systems and Technologies Conference (PEDSTC 2023), Babol, Iran.

[115] Ali Hussein Sultan; Harith Al-Badrani; «Modeling and Simulation of a Seven-Phase Induction Motor», Published in: 2023, International Conference on Engineering, Science and Advanced Technology (ICESAT-2023), Technical Engineering College / Mosul, Iraq, pp. 177-181.

[116] E. Levi, R. Bojoi, F. Profumo, H. A. Toliyat and S. Williamson, «Multiphase induction motor drives - a technology status review», Published in: 2007, IET Electric Power Applications, vol. 1, no. 4, pp. 489-516.

[117] Parekh Rakesh, «AC induction motor fundamentals», Published in: 2003, Microchip Technology Inc, pp. 1-24.

[118] Bahareh Anvari, Yonqgi Li, Hamid A. Toliyat, «Design of Multiphase Exterior Rotor Switched Reluctance Motor for Traction Applications » Published in: 2016 IEEE 25th International Symposium on Industrial Electronics (ISIE),pp. 161-166.

[119] Han, Shouyi, Diao, Kaikai, Sun, Xiaodong, « Overview of multi-phase switched reluctance motor drives for electric vehicles» Published in: Advances in Mechanical Engineering.

[120] Ahn, Jin-Woo, «Torque control» Published in: 2011,pp. 201-252.

[121] Edutecnica:Motore in corrente continua: Motore in corrente continua (edutecnica.it)

[122] A.V Zakharov; S.I Malafeev; A.L Dudulin« Synchronous reluctance motor: Design and experimental research» Published in: 2018 X International Conference on Electrical Power Drive Systems (ICEPDS).

[123] D. Cabezuelo; J. Andreu; I. Kortabarria; I. Mtz. de Alegría; E. Robles « Powertrain system of electric, hybrid and fuel cell vehicles: state of technology» Published in: 2017, IEEE 26th International Symposium on Industrial Electronics (ISIE)

[124] Wang, Zhikun, Ching, Herman,Huang, Shaojia,Wang, Hongtao,Xu, Tao,

«Challenges Faced by Electric Vehicle Motors and Their Solutions» Published in: 2021, IEEE Access. 9, Vol 9, pp.5228-5249.

[125] J. Guo, J. Wang, and B. Cao, « Regenerative braking strategy for electric vehicles, » Published in: 2009, in Proc. IEEE Intell. Vehicles Symp, pp. 864–868.

[126] «PMSM model» (R. Galluzzi, personal communication, October 24, 2022)

[127] Mohamed Amine Frikha, Julien Croonen, Kritika Deepak, Yassine Benômar ,Mohamed El Baghdadi, Omar Hegazy, « Multiphase Motors and Drive Systems for Electric Vehicle Powertrains: State of the Art Analysis and Future Trends» Published in: Energies 2023, 16, 768.

[128] Ali Emadi, Young Joo Lee, Kaushik Rajashekara«Power Electronics and Motor Drives in Electric, Hybrid Electric, and Plug-In Hybrid Electric Vehicles» Published in: 2008, IEEE Transactions On Industrial Electronics, Vol. 55, No. 6 pp.2238-2245.

[129] Jiawei Wang, «A Comparison between Si and SiC MOSFETs» Published in: 2020IOP Conference Series: Materials Science and Engineering.

[130] Juergen Biela; Mario Schweizer; Stefan Waffler; Johann W. Kolar, «SiC versus Si—Evaluation of Potentials for Performance Improvement of Inverter and DC–DC Converter Systems by SiC Power Semiconductors » Published in:2011, IEEE Transactions on Industrial Electronics ,Vol. 58, Issue: 7, pp. 2872 - 2882.

[131] Shahbaz Amin; Sahib Khan; Syed Sabir Hussain Bukhari, «A Comprehensive Review on Axial Flux Machines and Its Applications » Published in: 2019,International Conference on Computing, Mathematics and Engineering Technologies – iCoMET 2019

[132] Francesco Profumo, Zheng Zhang, and Alberto Tenconi,«Axial Flux Machines Drives: A New Viable Solution for Electric Cars » Published in:1997, IEEE Transactions On Industrial Electronics, VOL. 44, NO. 1, pp.39-45.